Chem Soc Rev

Fmoc-Modified Amino Acids and Short Peptides: Simple Bio-Inspired Building Blocks for the Fabrication of Functional Materials

Journal:	*Chemical Society Reviews*
Manuscript ID	CS-SYN-12-2015-000889.R2
Article Type:	Review Article
Date Submitted by the Author:	10-Apr-2016
Complete List of Authors:	Tao, Kai; Tel Aviv University, Molecular Microbiology and Biotechnology Levin, Aviad; Tel Aviv University Adler-Abramovich, Lihi; Tel Aviv University, Department of Molecular Microbiology and Biotechnology Gazit, Ehud; Tel Aviv University,

Chem Soc Rev

REVIEW ARTICLE

Fmoc-Modified Amino Acids and Short Peptides: Simple Bio-Inspired Building Blocks for the Fabrication of Functional Materials

Received 00th January 20xx,
Accepted 00th January 20xx

DOI: 10.1039/x0xx00000x

www.rsc.org/

Kai Tao,[a] Aviad Levin,[a] Lihi Adler-Abramovich[ab] and Ehud Gazit[*ac]

Amino acids and short peptides modified with the 9-fluorenylmethyloxycarbonyl (Fmoc) group possess eminent self-assembly features and show distinct potential for applications due to the inherent hydrophobicity and aromaticity of the Fmoc moiety which can promote building blocks association. Given the extensive study and numerous publications in this field, it is necessary to summarize the recent progress concerning these important bio-inspired building blocks. Therefore, in this review, we explore the self-organizations of this class of functional molecules from three aspects, *i.e.,* Fmoc-modified individual amino acids, Fmoc-modified di- and tripeptides, and Fmoc-modified tetra- and pentapeptides. The relevant properties and applications related to cell cultivation, bio-templating, optical, drug delivery, catalytic, therapeutic and antibiotic properties are subsequently summarized. Finally, some existing questions impeding the development of Fmoc-modified simple biomolecules are discussed, and corresponding strategies and outlooks are suggested.

1. Introduction

The self-assembly of biomolecular building blocks has been extensively studied owing to their inherent biocompatibility and ability to form nanostructures with diverse morphologies, along with possessing intriguing application potentials in a variety of fields.[1-6] Peptides composed of sequences shorter than five amino acids and even single amino acids have attracted a lot of interest due to their lower synthesis costs and relative ease of modulation compared to larger biomacromolecules.[4,7-10] By conjugating functional moieties, the modified self-assembly products can further offer unique and tunable morphologies of different functionalities, which provide a powerful tool for bio-soft matter fabrication. While the current progress of the study of modified short peptides that are stimuli-responsive,[11,12] or that bear naphthyl[13,14] and aliphatic tails[15,16] has been comprehensively reviewed, the self-organization and applications of Fmoc-modified simple biomolecules have not been extensively summarized.

Fmoc is widely used as a main amine protecting group in peptide synthesis.[17-19] The intrinsic hydrophobicity and aromaticity of Fmoc is well-known to promote the hydrophobic and π-π stacking interactions of the fluorenyl rings. Therefore, many Fmoc-modified amino acids and short peptides possess relatively rapid self-assembly kinetics and present remarkable physicochemical properties along with tremendous application potentials, such as cell cultivation, templating, optical devises, drug delivery, catalysis, therapeutic and antibiotics, as shown in Scheme 1.[20-23] Considering the increasing number of publications, herein we would like to introduce the recent progress on the self-assembly and relevant applications of this kind of multifunctional bio-inspired molecules.

2. The self-assembly of Fmoc-modified amino acids and short peptides

The self-assembly of peptide amphiphiles refers to a variety of non-covalent interactions, including hydrogen bonding, hydrophobic, aromatic interactions, and in some cases, electrostatic interactions.[24] The introduction of the Fmoc moiety can offer additional driving forces, such as hydrogen bonding from the carbonyl group,[25] other aromatic and hydrophobic interactions from the fluorenyl ring[20,26] and steric optimization from the linker (the methoxycarbonyl group)[21]. These unique interactions, along with the driving forces induced by the peptide sequences, result in the self-assembly of Fmoc-modified amino acids and short peptides in a kinetically rapid and thermodynamically rigid manner.

Among the Fmoc-modified biomolecules, those having sequences composed of amino acids with aromatic side-chains, such as phenylalanine (F), tyrosine (Y) and tryptophane (W), attract much interest. A previous study revealed that the Fmoc-modified biomolecules flanked with substantial aromatic moieties in their side-chains, such as Fmoc-β-(2-naphthyl)-

[a] Department of Molecular Microbiology and Biotechnology, George S. Wise Faculty of Life Sciences, Tel Aviv University, Tel Aviv, 6997801, Israel. E-mail: ehudg@post.tau.ac.il
[b] Department of Oral Biology, The Goldschleger School of Dental Medicine, Tel Aviv University, Tel Aviv, 69978, Israel.
[c] Department of Materials Science and Engineering, Iby and Aladar Fleischman Faculty of Engineering, Tel Aviv University, Tel Aviv, 6997801, Israel.

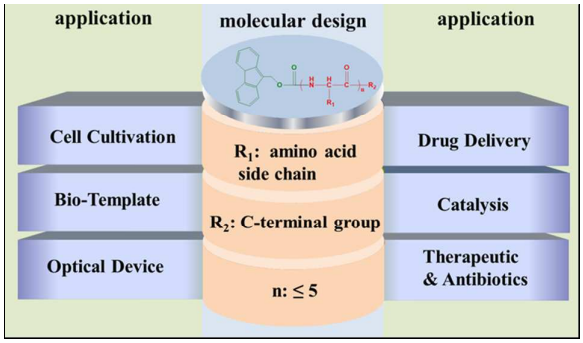

Scheme 1. Schematic representation showing the design principles and relevant applications of Fmoc-modified peptidic biomolecules. The introduction of the Fmoc group (green) promotes the self-assembly of amino acids or short peptides (red), which can be applied in a variety of advanced fields by modulating their molecular compositions, such as the amino acid residue numbers (n), side-chains (R_1) and C-terminal groups (R_2).

alanine (Fmoc-2-Nal) and Fmoc-FF, could self-assemble to nanofibrillar structures which then formed continuous viscoelastic hydrogels; while those with less aromatic side-chains, such as Fmoc-phenylalanine-proline (Fmoc-FP), Fmoc-phenylalanine-serine (*tert*-butyl) (Fmoc-FS(tBu)), Fmoc-arginine-glycine-aspartic acid (Fmoc-RGD) and Fmoc-GF, only aggregated into spherical or discrete tubular morphologies and remained viscous solutions.[27] An additional study demonstrated that a higher ratio of side-chain aromatic moieties could induce an elevated self-assembly yield, higher thermal stability, and elasticity of the formed hydrogels, and thus allowed a faster self-assembly process.[28] It is believed that the introduction of aromatic motifs at the side-chains allows a synergistic effect with Fmoc, forming π-π interactions both between Fmoc groups and side-chain phenyl rings, thus distinctly promoting the self-assembly. Therefore, studies on the self-association and application of Fmoc-modified biomolecules mostly focus on those with side-chain aromatic features.

2.1. Fmoc-Modified amino acids

Individual amino acids are among the simplest biomolecules allowing for Fmoc modification. Increasing Fmoc-modified amino acids have been reported to be able to self-assemble and some of them, mostly those with aromatic side-chains, can even form into extended three-dimensional (3-D) networks, trapping the solvent molecules and forming gels. Such gels can be employed as ideal low-molecular-weight hydrogelators, as shown in Table 1.[29-33] Of note is Fmoc-F, which is a leading hydrogelation promoter due to its excellent propensity to self-assemble.[29,] Other amino acids are mostly the derivatives of Fmoc-F, such as its fluorinated[30] and hydroxylated (Fmoc-Y[29,31,33] and its phosphorylated derivatives[31,33], Fmoc-DOPA[32,34]) derivatives.

Modifications of the phenyl group side-chain can significantly alter the mechanical properties of the hydrogel formed by Fmoc-F. For example, strong frequency-dependent moduli and highly flexible interconnections exist between junction zones in the Fmoc-F hydrogel networks, which can withstand large deformation.[29] When F was replaced with Y by conjugating a hydroxyl group at the *para*- position of the phenyl ring, Fmoc-Y self-assembled into a strong hydrogel with a higher storage modulus independent of the frequency applied.[29] Dynamic light scattering particle probe-based micro-rheology study indicated that the hydrogel formed by Fmoc-Y possessed molecule-level features which cannot be detected using electron microscopy, suggesting that the gel network exists on a broad length-scale, ranging from the angstrom to the micron size.[35] Presumably, the hydrogen bonding stemming from the side-chain phenolic rings and water molecules can promote the interlacing of the nanofibrils and solidify the solvent molecules, inducing the rigidity of the hydrogel. Furthermore, when replacing F with 3,4-dihydroxy-phenylalanine (DOPA), a catechol non-coded amino acid with a superior antioxidant property, Fmoc-DOPA aggregated linearly to form semi-flexible twisted-multi-stranded fibers at pH 2.0 by a heating-cooling cycle (from 70^o to 25^o), which disassembled at a higher pH due to the deprotonation of the carboxylic groups.[32] In addition, when using a solvent-switching strategy (ethanol stock solution dilution to water) while maintaining the solution at a lower temperature (18^o), the self-assembly dynamics of Fmoc-DOPA could be substantially slowed.[34] In this condition, a noninduced phase transitions from spherical assemblies to nanofibers followed by sol-gel transition, nanotube formation via intermediate assembly, and finally crystallization within the gel could be detected in detail.[34]

In addition to the hydroxyl groups, the incorporation of halogen substituents on the phenyl ring, including position (*ortho-, meta-, para-*), number (1-5) and the halogen atoms themselves (*F, Cl, Br*), can also exert a strong influence on the self-assembly of Fmoc-F.[36] For example, a previous study showed that among the *para*- halogen-substituted Fmoc-F derivatives, the most efficient gelator was Fmoc-*para*-fluoro-phenylalanine (Fmoc-(*4-F*)F), which could gelate at PBS buffer solution at the minimal gelation concentration of 0.15% (wt).[37] In contrast, Nilsson *et al.* found that Fmoc-pentafluoro-phenylalanine (Fmoc-*F5*-F, the five hydrogen atoms at the side-chain phenyl ring substituted by five fluorine atoms) could self-assemble to form a hydrogel within minutes at room temperature at a concentration of only 0.1% (wt), with much higher viscoelastic rigidity than that of Fmoc-Y.[38] A comparison of the self-assembly of fluorinated Fmoc-F molecules with their corresponding C-terminal amidated and methyl derivatives found that the ester derivatives failed to form hydrogels due to their high hydrophobicity, while the amidated derivatives aggregated much more rapidly, but the resultant hydrogels were unstable during shear stress. It is plausible that the amide bonds cannot form extensive hydrogen bonding compared to carboxyl groups due to their relative inertness, resulting from the *p*-π conjugation between the nitrogen atom and the carbonyl bond.[30]

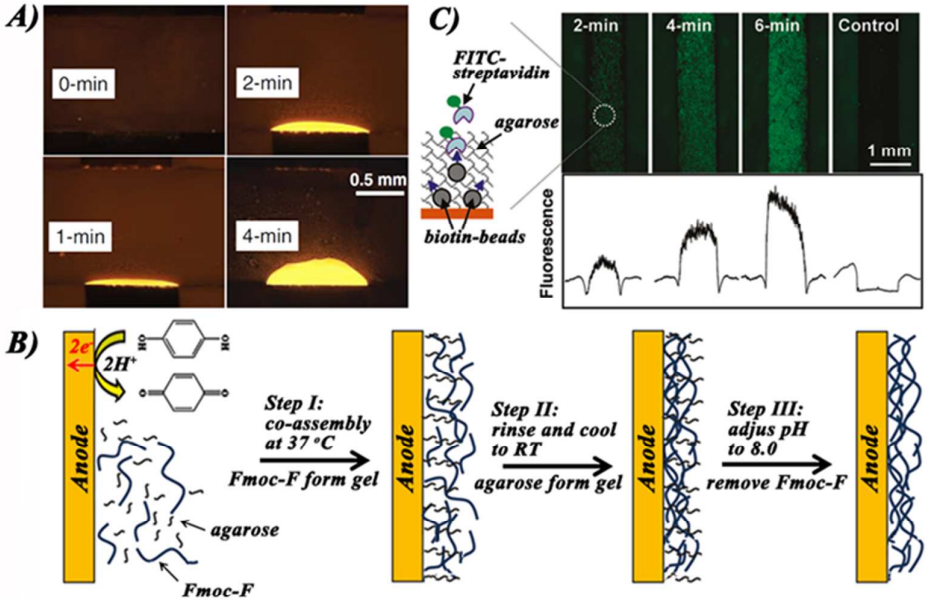

Figure 1. (A) Fluorescent micrograph showing the Fmoc-F gelated film electrodeposited on an electrode, with thickness tuned by controlling the deposition time. (Reproduced with permission from [40]. Copyright 2011 Wiley-VCH Verlag GmbH & Co. KGaA, Weinheim). (B) Schematic representation showing the mechanism of electrochemically co-depositing agarose using Fmoc-F gelated film on the electrode (Reproduced with permission from [39]. Copyright 2011 American Chemical Society). (C) Fluorescent micrograph showing the FITC-modified streptavidin bound to the biotin-functionalized microparticles deposited in the agarose gel, with amounts tuned in a time controlled manner. (Reproduced with permission from [39]. Copyright 2011 American Chemical Society).

Electrochemical technique offers a new approach to control the self-assembly of Fmoc-modified single amino acids. In a previous work by Payne and co-workers, through the electrochemical oxidation of hydroquinone to 1,4-benzoquinone, the release of protons decreased the pH to a small extent, allowing Fmoc-F molecules to be deposited and to self-assemble to form a nanofibrillar hydrogel film in a localized area of the electrode.[39] The thickness of the film could be tuned with time and the whole progress was reversible by adjusting the pH, as shown in Figure 1A.[40] The rapid assembly and disassembly kinetics could be spatially controllable, which can be utilized for lab-on-a-chip applications.[40] For example, through co-deposition of a thermally responsive polysaccharide agarose at 37 °C, followed by cooling to room temperature to induce gelation, and finally adjustment to a neutral pH to disassemble the Fmoc-F hydrogel, an agarose gel could be prepared at the electrode, as shown in Figure 1B.[39] The prepared agarose gel could be further utilized to co-deposit other functional composites, such as biotin-modified beads, thus specifically recognizing, detecting, and addressing a corresponding epitope, *i.e.,* streptavidin, as shown in Figure 1C.[39] Furthermore, electrochemical co-deposition of gelatin using Fmoc-F could produce a gel which can transit to a sol when the temperature was adjusted from 37 °C to 22 °C.[41]

The co-assembly strategy can endow diverse functionalities to the self-assemblies.[23,42,43] Co-assembly of Fmoc-leucine (Fmoc-L) and Fmoc-ε-lysine (Fmoc-$^{\varepsilon}$K, the side-chain ε-amino group modified with Fmoc) could form a supermolecular hydrogel possessing anti-inflammatory properties,[44] while the introduction of pamidronate, a biomedical agent, could produce a multicomponent hydrogel useful for treatment of the toxicity of uranyl oxide at wound sites.[45] Moreover, a suspension solution of Fmoc-$^{\varepsilon}$K and Fmoc-F could transit to a hydrogel with an exceptionally high storage modulus and excellent elasticity upon a heating-cooling cycle in the presence of Na_2CO_3.[46] Further through combining the heme model compounds with the hydrogel, an artificial peroxidase with catalytic activity could be prepared. This composite hydrogel can be easily tailored by controlling the distal substituents above the coordinated centres of the heme model compounds.[47]

It is plausible that the co-assembly of different halogen-substituted Fmoc-F molecules can produce much more rigid hydrogels. For example, co-assembly of Fmoc-*F5*-F and C-terminal PEG-functionalized Fmoc-*F5*-F (Fmoc-*F5*-F-PEG) could form a hydrogel which was stable with respect to shear-response and exhibited ideal stress-responsive behaviors.[48] Co-assembly of Fmoc-F and Fmoc-*F5*-F, with side-chain groups of complementary quadrupole electronics, could also form two-component nanofibrillar hydrogels under conditions in which Fmoc-F alone fails to self-assemble.[49]

The combination of co-assembly strategies and electrostatic attractive interactions can produce unique Fmoc-modified amino acids self-assemblies. When equimolarly mixing the oppositely charged Fmoc-*L*-glutamic acid (Fmoc-*L*E) and Fmoc-*L*K, the electrostatic attractive interactions induced the two building blocks to co-assemble to form left-handed

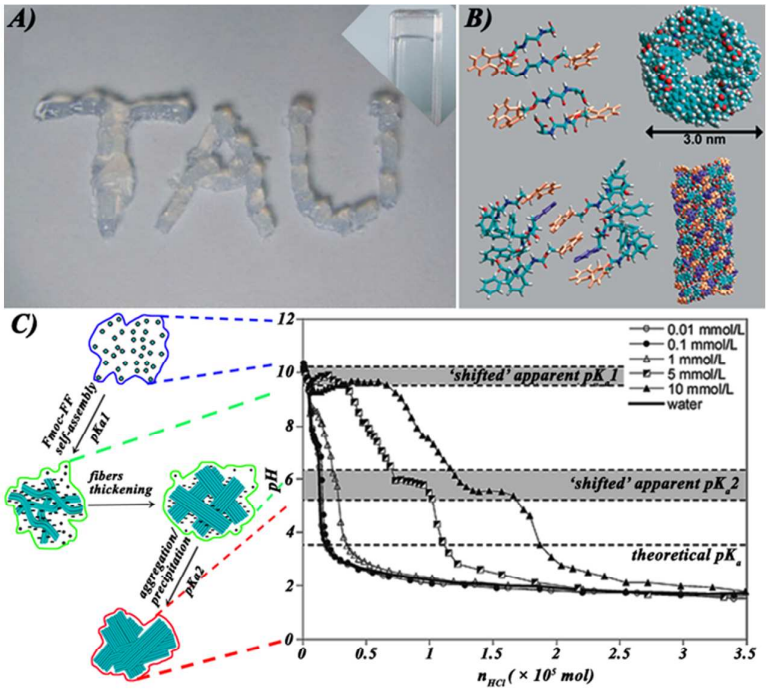

Figure 2. Self-assembly and hydrogelation of Fmoc-FF. (A) Picture showing the letters TAU (Tel Aviv University) written by the Fmoc-FF hydrogel. The inset presenting that the hydrogel remains stable in the inverted cuvette. (Reproduced with permission from [20]. Copyright 2006 Wiley-VCH Verlag GmbH & Co. KGaA, Weinheim) (B) Model structures representing the molecular arrangements during Fmoc-FF self-assembly. Note that the fluorenyl and phenyl groups are separately coloured orange and purple to illustrate the paired π -stacking nature of the aromatic moieties during self-assembly. (Reproduced with permission from [26]. Copyright 2008 Wiley-VCH Verlag GmbH & Co. KGaA, Weinheim) (C) pH evolution *vs.* HCl titration (right panel) and a scheme (left panel) showing the different self-assembly process of Fmoc-FF inducing different phenotypical pK_a. (Reproduced with permission from [61]. Copyright 2009 American Chemical Society)

nanofibrillar hydrogels.[50] While the conformation of the nanofibers was right-handed when using *D*-isomers as building blocks, suggesting that the molecular chirality can be translated into the supermolecular helicity and the handedness of these nanofibers depends on the corresponding component chirality in the co-assembly system.[50]

In addition to co-assembly, covalent conjugation presents another approach to the functionalization of self-assemblies. The conjugation of stearamine to the C-terminus of Fmoc-G could provide a new compound named FGC18 to self-assemble into nanofibrillar organogels in some organic solvents at a lower temperature (-15 °C).[51] Interestingly, the nanofibers could transform into dendritic twists and then to giant microbelts in ambient temperature, and the process was found to be reversible upon dilution of the organogel.[51] Furthermore, through co-assembly of FGC18 and its chiral alanine (A) analogues, *i.e.,* *L*-type and *D*-type FAC18, nanotwists with uniform chirality could be obtained.[51] Besides, conjugation of poly(2-isopropyl-2-oxazoline) (PiPrOx), a thermal responsive polymer, to Fmoc-modified amino acids could design several Fmoc-amino acid-PiPrOx molecules to self-assemble to form temperature-responsive colloidal particles.[33] By increasing the temperature from room temperature to above the lower critical solution temperature (LCST), a phase transition from solution phase of these conjugates to precipitates could be induced.[33] Moreover, the types of amino acids, such as Fmoc-F or Fmoc-Y, could drastically influence the self-assembly behaviors.[33]

2.2. Fmoc-Modified di- and tripeptides

Compared to the individual amino acids or longer oligopeptides, di- and tripeptides have attracted much more interest in the field of biomolecular self-assembly due to their flexible and tunable molecular structures, notable mechanical properties, along with the cost-effectiveness.[4,7,10,52-56] Thus, Fmoc-modified di- and tripeptides have been extensively studied owing to their excellent self-assembly properties, as shown in Table 1.[20,26,57,58]

2.2.1. Fmoc-Modified diphenylalanine. The most extensively studied Fmoc-modified dipeptide is Fmoc-FF, which is derived from the core recognition motif of Alzheimer's disease-associated β-amyloid polypeptide.[59] Since it was first found to form rigid hydrogels,[20,26] as shown in Figure 2A, the self-assembly and relevant applications of Fmoc-FF have become pivotal in various bio-soft matter fields.[60-62] Studies have confirmed that during self-assembly, Fmoc-FF molecules forms cylindrical nanofibrils by interlocking four twisted antiparallel β-sheets through lateral antiparallel π-π interactions,[26] as shown in Figure 2B; and the self-assembly process can result in two phenotypical pK_a values: one located at pH 9.5-10.2,

corresponding to the self-assembly of both protonated and non-protonated molecules into nanofibrils, and the other one located at pH 5.2-6.2, related to massive aggregation of the nanoribbons, triggered by further neutralization of the molecules, as shown in Figure 2C.[61]

While through slow acidification of the aqueous solution encapsulated by the liquid marble of *Lycopodium clavatum* spores with gaseous carbon dioxide, Fmoc-FF could self-assemble to an ultrathin (thickness of 50-500 nm) interwoven membrane of ribbon-like fibers at the liquid/air interface.[63] The meshed membrane could incorporate the lycopodium microparticles, thus stabilizing the liquid marble against collapse.[63] Interestingly, the electron diffraction analysis indicated that the cylindrical nanofibrillar model presented above could not perfectly explain the arrangements of the biomolecular entities in the membrane; instead, a planar compact columns stacking model could offer an interpretation.[63] This implies on the complicated self-assembly process of Fmoc-FF that still attracts a great research interest in this minimal motif. In addition, a series of orthogonal experiments to change the hydrogelation conditions demonstrated that the final pH in which assembly takes place is the principal determinant for the mechanical properties of Fmoc-FF hydrogels,[60] while other experimental factors, such as the ratio of organic solvent to water[60,64] and the buffers used,[60] affect the rheological properties to a lesser extent. Moreover, the homogenization techniques used during the gelation process, such as vortex *vs.* manual agitation, can also dramatically influence the structural and mechanical properties of the hydrogels formed, with variations of up to one order of magnitude in shear modulus.[65]

All these findings indicate that the self-association process and underlying mechanism of Fmoc-modified biomolecules are significantly complicated and there are still a lot remaining to be clarified. Therefore, we would suggest that in future Fmoc-modified self-assembly studies, all possible influencing factors, including the biomolecular structures, solvent compositions (solvent type and polarity, ratio of organic solvent to water, buffer components), solution conditions (ionic type and valence state, ionic strength, pH) and external conditions (temperature, homogenization method), should be thoroughly considered.

Co-assembly with other composites offers a simple approach to modulate the self-assembly and hydrogelation of Fmoc-FF. For example, co-assembly of Fmoc-FF and Fmoc-modified single amino acids (K, D and S)[66] or functional peptide motif (RGD),[67] could produce hydrogels with composition-dependent elastic moduli, ranging from 502 Pa (Fmoc-FF+ Fmoc-D) to 21200 Pa (Fmoc-FF alone).[66] In addition, in Fmoc-FF co-assemblies with dextran additives, the dextran types and the absolute viscosity of the solutions could have a substantial effect on the rheological properties of the final gels.[68] Specifically, when the solution viscosity was below 8 mPas, the rheological properties were similar, but in all cases were lower than that of the Fmoc-FF gel itself. When the viscosity was higher than 8 mPas, the formed gels became progressively weaker, resulting from a decrease in spherulite size and entanglements relative to Fmoc-FF gel.[68]

2.2.2. Fmoc-Modified tyrosine-leucine dipeptide. Fmoc-YL is another Fmoc-modified dipeptide that has been extensively studied because of its ease of modulation and functionalization. For instance, anions could greatly affect the hydrogelation of Fmoc-YL, leading to the transformation of the supermolecular structures from densely fibrous networks to spherical aggregates, accompanied by variations in the elastic moduli (G') of the hydrogels from 0.8 kPa to 2.4 kPa.[69] The efficiency of the anion types is consistent with the Hofmeister anion sequence.[69] Interestingly, the affecting mechanism results from the specific ion effects on the structures of the gels rather than the sol-gel equilibrium.[69] This specific ion dependency, combining with the enzyme-catalytic self-assembly strategy which will be discussed below, can give rise to more complex self-assembly behaviors.[70]

Ultrasonication can also be used to control the self-assembly of Fmoc-YL. Ultrasonic waves could enhance the stacking interactions of the fluorenyl rings while having a less effect on hydrogen bonding, which caused the ordered nanotapes formed by Fmoc-FL to transform into coiled nanofibers and disrupted the fibrillar network to form spherical aggregates. It should be noted that this transition could be reversible in the absence of sonication.[71]

Fmoc-YL could also self-assemble at the organic/aqueous interface to emulsify and stabilize the water/oil emulsions.[72] The system could maintain long-term stability even at a high temperature (60 ^{o}C) or salt concentration (100 mM), but could be easily demulsified by thermolysin-triggered disassembly at physiological conditions.[72]

The linker between the fluorenyl moiety and the YL dipeptide also has a significant impact on the self-assembly and hydrogelation process. The more rigid linkers facilitate the hydrogelation while the shorter linkers restrict the conformation and aromatic stacking interactions.[21] By comparison, the Fmoc group, carrying a methoxycarbonyl group, seemed to be the optimal choice for the hydrogelation of YL, providing a rigid linker of sufficient length to allow effective assembly for both the aromatic and dipeptide domains.[21] It is probable that this linker allows for Fmoc-modified biomolecules to generally possess excellent self-assembly and hydrogelation properties.

Co-assembly strategies can also be utilized to adjust the self-assembly of Fmoc-YL.[73] For example, a cooperative type of co-assembly of Fmoc-YL with pyrene-modified YL (Pyr-YL) could allow these bio-inspired building blocks to share their common propensity to form β-sheet secondary structures. In contrast, disruptive types of co-assembly of Fmoc-YL with Fmoc-S could only allow these molecules to share the same aromatic moiety, resulting in the substantial intercalation of the S component and ultimately compromising the β-sheet arrangement

integrity of YL. Moreover, an orthogonal type of co-assembly of Fmoc-YL and Pyr-S, achievable only when every segment of each component is sufficiently different from the other, could not disrupt the respective β-sheet arrangements.[73]

2.2.3. Other Fmoc-modified di- and tripeptides. Along with FF and YL, other Fmoc-modified di- and tripeptides, mainly inspired from modifications of Fmoc-FF or Fmoc-YL, also possess interesting self-assembly properties. For example, Fmoc-FG, GG, GF, LL, LG and GL, analogues of Fmoc-FF and Fmoc-YL, also showed substantially shifted apparent pK_a transitions during their self-assembly, accompanied by the self-assembling morphological changes.[74,75] The fact that the replacements of the sequence does not affect the propensity of the Fmoc-modified dipeptides to self-assemble into fibrillar structures clearly points toward the key role of the Fmoc group and to π-π interactions in driving the self-assembly of these systems.[75] Therefore, it can be concluded that the main driving force behind the self-assembly process of Fmoc-modified short peptides is a combination of the fluorenyl hydrophobic and π-π interactions, with a secondary role for hydrogen bonding.[74]

Similarly to the aforementioned Fmoc-DOPA, Fmoc-[DOPA][DOPA] dipeptide could also self-organize into fibrillar hydrogels, displaying high catechol group density on the surface which could spontaneously reduce and assemble metal cations to form 1-D nanowires.[76] Furthermore, by introduction of a K to the C-terminal, Fmoc-[DOPA][DOPA]K tripeptide was synthesized to self-assemble to nanostructures which possessed exceptional glue-like properties.[76] Another study showed that Fmoc-KK, with the side-chain ε-amino group of C-terminal K functionalized with the *n*-type 1,4,5,8-naphthalenetetracarboxylic acid diimide (NDI) chromophore, could self-assemble to form nanobelt-based, self-supporting transparent hydrogels.[77] The intermolecular π-π delocalization of the NDI units along the long axis and of the fluorenyl groups along the lateral dimension was anticipated to mediate the long-range charge migration for applications in the optoelectronic and biomedical fields.[78]

The conversion of peptide sequences can offer an additional approach for controlling the self-assembly of Fmoc-modified short peptides. For example, Fmoc-valine-leucine-lysine (N^{ε} modified with *tert*-butyloxycarbonyl) (VLK(Boc)) was found to self-assemble to form amyloid-like β-sheets secondary structures, producing highly anisotropic fibrous hydrogels. After inversion of the peptide sequence, Fmoc-K(Boc)LV self-assembled into highly branched fibrils with multiple stacked sheets that produced isotropic hydrogels with a much higher shear modulus (G' > 104 Pa).[79]

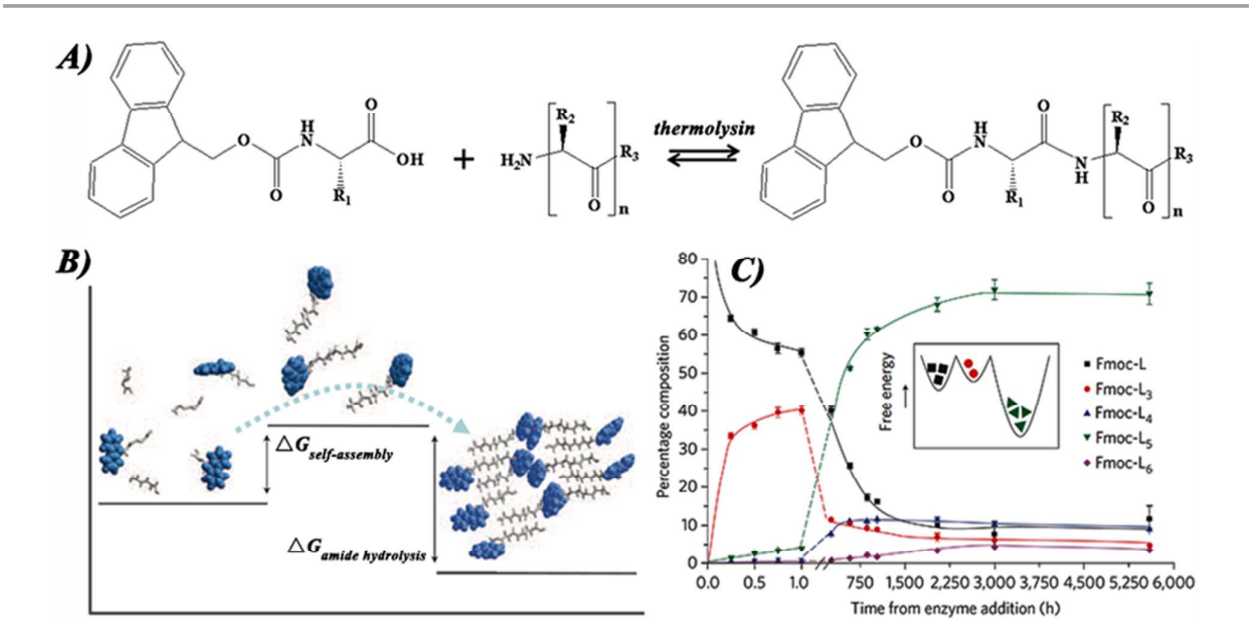

Figure 3. Enzyme-Catalytic self-assembly of Fmoc-modified biomolecules. (A) Chemical reaction equation illustrating how Fmoc-modified peptidic building blocks are synthesized by thermolysin-catalytic coupling reactions. R_1 and R_2 denote side-chains, R_3 denotes methyl ester or hydroxyl group. (B) A diagram showing the mechanism underlying the enzyme-assisted DCL used to identify the thermodynamically stable self-assemblies of Fmoc-modified biomolecules. The Fmoc group and peptide sequence is marked in blue and grey colour, respectively. (C) An HPLC profile *vs.* time indicating the re-distribution of Fmoc-modified building blocks synthesized from thermolysin-catalytic coupling of Fmoc-L and LL. (Reproduced with permission from [94]. Copyright 2008 Nature Publishing Group)

The electrochemical technique described above can also be applied to induce the self-assembly of other Fmoc-modified di- and tripeptides, using the same mechanism as that for Fmoc-F. For example, in an original work by Adams and co-workers, the Fmoc-LG solution could undergo localized sol-gel transition to form gelated films at metallic substrates through the decrease

Table 1. Summary of the reported Fmoc-modified amino acid and short peptide sequences

Biomolecular Sequences	Self-Assembly Profiles or Functionalities	References
	Single Amino Acid	
F/(halogen)F//F-Se	nanofibrillar hydrogels//nanospheres to nanotubes through oxidation	29,35,39-41,46/30,36-38, 48,49//155
Y/(p)Y//DOPA	nanofibrillar hydrogels	29,35,85/31,167//32,34
F-PiPrOx, Y-PiPrOx, K-PiPrOx	nanofibrillar hydrogels	33
L+$^{\varepsilon}$K/Y+$^{\varepsilon}$K//F+$^{\varepsilon}$K	nanofibrillar hydrogels//suspension to nanofibrillar hydrogels	44,45/167//46,47
E+K, E+O, E+R	left-/right-handed nanofibers for *L*/*D*-type isomers	50
L	anti-inflammatory	162
S	nanospheres	85
G-stearamine/(octyl)G	nanofibers to nanotwists to nanobelts/deposits of unbranched nanowires to nanofibrillar hydrogels	51/83
	Dipeptide	
FF/F(*para*-X)F-NH_2	nanofibrillar hydrogels/wider sheets or tubes when X is electron-donating group, while narrow nanofibers when X is electron-withdrawing group	20,26,49,60-68,72,86,108,111, 118,138,63/96
FY/F(p)Y	nanofibers/micelles	100,101,165/100,101
FL	nanotapes transform to coiled nanofibers	71
FC/CF-OMe	stabilizer of other Fmoc-modified nanospheres/nanofibrillar hydrogels	150/98
GG, FG/GF	nanofibrillar hydrogels/sheet-like precipitates	65,74,81
GS, GT, GA	nanofibrillar hydrogels	81
YL	nanofibrillar hydrogels with different order, chirality or mechanical properties	21,69-73, 102
YA, YS	microcapsules with nanofibrillar networks at the organic/aqueous interface	72
[DOPA][DOPA]	nanofibrillar hydrogels	76
YT, YS, YN/YQ	nanofibrillar hydrogels/nanospheres	91,165
SF-OMe, SL-OMe/TF-OMe, TL-OMe	nanoplanar hydrogels/twisted-ribbon hydrogels	90,97/90
VV/TF-OMe, TL-OMe	nanofibrillar hydrogels	95
LL//LL-benzoyl	nanofibrillar hydrogels/sol-gel transition by addition of anions//sheet-like particles to nanofibrillar hydrogels	58,75,95/69//82

Biomolecular Sequences	Self-Assembly Profiles or Functionalities	References
LG/VL	nanofibrillar hydrogels/sol-gel transition by addition of anions	58,75,103/69
LD	nanofibrillar hydrogels	148
KK(NDI)-NH_2	flat nanobelt hydrogels	77,78
AA	nanofibrillar hydrogels to sol/nanofibrillar hydrogels	81/25,84
	Tripeptide	
FFF	microcapsules with nanofibrillar networks at the organic-aqueous interface/nanofibrillar hydrogels	72/99
FFH	nanotubes	154
LLL	nanotubes/nanofibers	93,95/94,95
RGD	nanofibrillar hydrogels	67,109,111
VLK(Boc)/K(Boc)LV	nanofibers/highly branched nanofibers	79
FWK	nanofibers to nanoribbons to nanohelices to nanofibers	80
WFF	inhibitor of mRR	163
[DOPA][DOPA]K	nanofibers	76
E(p)YL	affinity to PTP	164
	Tetrapeptide	
RGDS, GRDS	nanofibrillar hydrogels	105,106,110,124
RGDF, FRGD	nanofibrillar hydrogels	27,28
	Pentapeptide	
KGG*D*A*D*A	aggregates	57
VTEEI, GVGVP, VPGVG, VYGGG	nanofibrillar hydrogels	107
FFECG	nanofibers	119
LLLLL	sheet-like structures	94

Se: selenium; p: Phosphorylated; PiPrOx: poly(2-isopropyl-2-oxazoline); $^{\varepsilon}$K: the side-chain ε-amino group of lysine; OMe: methoxy group; NDI: 1,4,5,8-naphthalenetetracarboxylic acid diimide;
Parentheses: modification to side-chain; Short transverse line: modification to C-terminus of backbone

of the pH.[58] And the films could be dried to collapse, then re-swollen to recover the gel structure again.[58] Notably, the film structures, *i.e.,* thickness and components, can be easily tuned by controlling the deposition conditions, such as the final pH, the rate of the decrease of pH, and the dipeptide sequences.[58]

Electrostatic interactions can also be utilized to control the self-assembly of Fmoc-modified bio-building blocks. For instance, Fmoc-FWK tripeptide could self-assemble to form nanofibrils at pH 5.0, which transformed to larger flat ribbons composed of many nanofibers as pH increased to 6-11, then twisted into left-handed helices at pH 11.2-11.8, and finally back to nanofibrils when pH was extremely basic (pH 12.0).[80] Structural characterizations revealed that the electrostatic interactions between the charged carboxyl and amino groups at K residues played an important role in directing the assembly process. As a control, when blocking one of the charged groups, such as C-terminal amidation, Fmoc-FWK-NH_2 only self-assembled to form stable nanofibrils regardless of the solution pH.[80] It is assumed that at acidic pH (pH less than the pK_a of the carboxyl groups, where carboxyl and amino groups

are both protonated), stronger electrostatic repulsive interactions from positively-charged amino groups induce the self-assemblies to twist into nanofibrils. When pH is increased to 6-11, where both carboxyl and amino groups are charged, the thinner nanofibrils aggregate laterally to form wider nanoribbons with electrostatic attractive interactions. And when pH is further increased to 11.2-11.8, which is near the pK_a of the amino groups, stronger electrostatic repulsive interactions from negatively charged carboxyl groups lead to the nanoribbons twist into nanohelices, which finally decompose into individual nanofibrils again when pH reaches to 12.0.

Specific ligand-receptor interactions can be used as another tool for controlling the Fmoc-modified self-assemblies.[81] The nanofibrillar hydrogel formed by Fmoc-*D*A*D*A dipeptide could convert to a sol through the introduction of vancomycin (Van) to disrupt the delicate balance between the hydrophobic interactions and the hydrogen bonds via ligand-receptor interactions. Conversely, its enantiomer, Fmoc-*L*A*L*A, lacking a specific recognition property for Van, showed no such response.[57] Furthermore, this specific ligand-receptor interaction could catalyse Fmoc-KGG*D*A*D*A, a pentapeptidic derivative of Fmoc-*D*A*D*A, to aggregate by a binding → propagation → dissociation → autocatalysis → aggregation process.[57] In contrast, Fmoc-KGG*L*A*L*A or KGG*D*A*D*A only resulted in inactive compounds, implying that the aromatic and ligand-receptor interactions are both responsible for the aggregation.[57]

The ultrasonication technique described above can also be used to control the self-assembly of other Fmoc-modified di- and tripeptides. For instance, C-terminal benzoyl-modified Fmoc-LL (Fmoc-LL-benzoyl) aggregated to sheet-like particles through a heating-cooling cycle in alkane solvents. While when subjected to ultrasound, the morphologies reshaped to elongated 3-D hydrogel networks of nanofibers or nanoribbons.[82] Furthermore, the side-chain octyl group conjugated Fmoc-G (Fmoc-OG) self-assembled to form deposits comprising of large numbers of unbranched nanowires in cyclohexane through a heating-cooling cycle. Yet, following the ultrasonic treatment, the deposits also transformed to entangled fibrous hydrogel networks. Further studies elucidated that the ratio between the Fmoc-OG molecules in a stable intramolecular H-bonding conformation and those in a metastable intermolecular H-bonding conformation could be tuned by the ultrasound; and the increased population of the intermolecular H-bonding induced by ultrasonication facilitated the interconnection of nanofibers for the formation of a fibrous network, and therefore gelation.[83]

Molecular simulation can act as a complementary approach to experimental techniques for studying the self-assembly of Fmoc-modified biomolecules. Computational simulations showed that during self-assembly, Fmoc-AA molecules converged into condensed fibrillar structures in which Fmoc groups mostly stacked within the center of the fibril, consistent with the normally-believed molecular structures. Moreover, along with the Fmoc stacking and inter-residue hydrogen bonding, hydrogen bonding between Fmoc-AA and water molecules also played an important role in stabilizing the self-assemblies.[84] However, the simulation also indicated that the AA sequence mainly adopted extended polyproline II conformation secondary structures, rather than the commonly hypothesized β-sheet conformation.[84] This discrepancy may arise from the inappropriate parameters used for simulations, but is more likely caused by the different self-assembly approaches, which implies the complex nature behind the Fmoc-modified self-assemblies. To balance the hydrophilic and hydrophobic nature and more effectively simulate the self-assembly behaviours of Fmoc-modified biomolecules, a modified parameterization protocol for the CHARMM force field used in molecular dynamics simulations was developed. The derived parameters for the Fmoc moiety from this updated algorithm were shown to be able to re-configurate the intermolecular interactions by reproducing quantum mechanical (QM) binding energies between the Fmoc group and water and between two Fmoc moieties, and to reproduce the flexibility of the Fmoc group by comparing dihedral distributions in MD simulations and their MM energetic profile with the corresponding QM dihedral scans.[85] Furthermore, the Fmoc parameterization successfully reproduced the thermodynamic parameters and self-assembling of Fmoc-S nanospheres and Fmoc-Y nanofibers , consistent with the experimental findings, confirming the validity of the modified parameterization protocol.[85]

It should be noted that despite the extensive progress in this field, it is still difficult to elucidate in a detailed fashion, the specific link between the molecular structures and the gel properties during the self-assembly of Fmoc-modified short peptides. This suggests that the hydrogels are likely determined not only by the molecules used and the final solution conditions, but also the route and kinetics used to reach those conditions.[86]

2.2.4. Enzyme-Triggered self-assembly of Fmoc-modified short peptides. The introduction of enzymes opens up an interesting method of controlling the Fmoc-modified bio-assemblies by conversions between self-assembling building blocks and their non-assembling counterparts.[8,11,12,23,87-89] These supermolecular morphologies are highly tunable, depending on the compositions,[90,91] sequence lengths[92,93] and the free energy landscapes of the self-assemblies.[94]

2.2.4.1. Thermodynamically driven self-assembly using biocatalysis

In a pioneering work, Ulijn and co-workers showed that thermolysin, a hydrolysis protease, could be used to trigger the self-assembly of Fmoc-modified peptidic building blocks. By harnessing the reversibility of thermolysin-catalytic peptide bonds hydrolysis, a series of Fmoc-modified individual amino acids and dipeptides were coupled to Fmoc-tripeptides, which could self-assemble to form high-order aggregates driven by π-

π interactions between fluorenyl groups, as shown in Figure 3A.[92,95]

Fmoc-(*4-X*)FF-NH_2, a Fmoc-FF derivative synthesized by thermolysin-catalytic coupling of Fmoc-(*4-X*)F and F-NH_2, could self-assemble to form diverse morphologies by controlling the X substituents.[96] Specifically, when X represented an electron donating group, such as -OH and -OPO_3H_2, sheet-like or tubular nanostructures were self-assembled; but when X represented an electron withdrawing group (-F, -CN and -NO_2), nanofibrillar structures were formed. It is plausible that the electron-donating groups can boost the delocalization of π-electrons and increase the aromaticity of phenyl rings, promoting the lateral aromatic interactions which finally lead to wider nanostructures formation; while the electron-withdrawing groups could impede the delocalization of π-electrons and impair the aromaticity of phenyl rings, resulting in weaker lateral aggregation interactions.[96] Another Fmoc-modified dipeptide, Fmoc-SF methyl ester (Fmoc-SF-OMe), formed by thermolysin-catalysed condensation of Fmoc-S and F-OMe, could self-assemble in a pair-wise manner to form β-sheets secondary structures which present either phenyl or hydroxyl functionalities at one side. These β-sheets could laterally self-assemble to form thermodynamically stable extended sheets over kinetically favored 1-D structures to shield the hydrophobic face from the aqueous environment.[97]

In fact, the strategy of thermolysin-triggered Fmoc-modified biomolecular self-assembly can be further used to develop dynamic combinatorial libraries (DCL) to identify stable self-assemblies through thermodynamically driven component selections. This is due to the fact that the amide formation is thermodynamically unfavored ($\Delta G_{amide\ hydrolysis}$) and will occur only when the building blocks form thermodynamically more stable structures ($\Delta G_{self\text{-}assembly}$), as shown in Figure 3B.[94] For example, Fmoc-threonine (Fmoc-T) and L-OMe could be conjugated to Fmoc-TL-OMe dipeptide with thermolysin. However, following the introduction of F-OMe to the system, Fmoc-TF-OMe dominated the self-assembling dipeptides. Furthermore, when a solution of Fmoc-L was coupled with LL in a 5 hours reaction catalysed by thermolysin, Fmoc-LLL (Fmoc-L3) tripeptide, which can self-assemble to form nanofibrillar structures, dominated the products with a yield of approximately 47%; as the reaction continued, Fmoc-LLLLL (Fmoc-L5) became the dominant form and yielded up to 70% after reacting for 5600 hours, accompanied with a transition of the self-assemblies to sheet-like structures, as shown in Figure 3C.[94] Utilizing this unique DCL strategy, Fmoc-CF-OMe could be dominantly synthesized through thermolysin-catalytic coupling of Fmoc-C and F-OMe in anaerobic conditions, which finally self-assembled to form a nanofibrillar hydrogel.[98] The hydrogelation can allow for a unique control of the system that is able to 'lock' a specific functional state of a dynamic library, thus not only preventing oxidation of the oxygen-sensitive thiol groups, but stopping the dynamic processes from reaching equilibrium.[98]

Lipase is another enzyme used to trigger the self-assembly of Fmoc-modified bio-building blocks via a reverse hydrolysis mechanism similar to thermolysin. For example, the lipase extracted from *P. cepacia* could be used to conjugate Fmoc-F and FF to Fmoc-FFF tripeptides which could self-assemble to form hydrogels with a porous microstructure at a lower concentration (1.36 mg ml^{-1}).[99] Due to their innate biocompatibility and porosity, which allow for cell mobility and nutrient diffusion, these hydrogels make attractive matrixes for 3-D cell cultivation in the field of tissue engineering.[99]

Subtilisin, an ester-hydrolysis enzyme, can also be used to trigger the Fmoc-modified self-assemblies.[95] For instance, the effects of the C-terminal amino acid's side chain on the molecular packing abilities were investigated with the help of subtilisin-catalytic hydrolysis of corresponding methyl esters of four closely related Fmoc-dipeptides, *i.e.,* Fmoc-YT, Fmoc-YS, Fmoc-YN, and Fmoc-YQ. Results showed that the first three dipeptides formed nanoscale fibers with mechanical properties linked to the functionality of the amino acid side-chain; while Fmoc-YQ formed spherical structures, probably due to the steric effects of the glutamine side chain prohibiting the adoption of the typical π-β assembly.[91] While Fmoc-LLL, which was derived from the hydrolysis of the corresponding methyl ester by subtilisin, could self-assemble to form nanotubular networks that were locked together via π-π stacking interactions.[93] Due to the short π-π stacking distance between the fluorenyl groups (3.6-3.8 Å), the nanotubular xerogel networks possessed distinct conductivity, with a minimum sheet resistance of 0.1 MΩ sq^{-1} in air and 500 MΩ sq^{-1} under vacuum (pressure of 1.03 mbar) at room temperature.[93]

Another enzyme that could be used to trigger the self-assembly of Fmoc-modified biomolecules is phosphatase, which can deprotect the phosphoric group from hydroxyl-containing amino acids, such as Y, S and T.[31] For example, side-chain phosphorylated Fmoc-FY dipeptide (Fmoc-F(p)Y), which formed micellar structures in solution, was dephosphorylated to form Fmoc-FY which could self-assemble into nanofibrillar hydrogels after treatment with phosphatase.[100] Furthermore, dephosphorylated Fmoc-FY could self-assemble to form metastable nanoparticles using reverse microemulsion as templates, which gradually transformed to thermodynamically stable nanotubes over time.[101]

As has been demonstrated by biocatalysis-induced self-assembly using C-terminal ester hydrolysis and side-chain dephosphorylation, it can be concluded that the C-terminal and side-chain modifications of peptide sequences play important structural roles in Fmoc-modified self-assemblies, along with the innate peptidic sequences. Therefore, when studying the self-association of Fmoc-modified building blocks, the C-terminal and side-chain structures should also be considered in detail.

It should be noted that, besides enzyme-triggered transformation from non-assembling precursors to self-assembling building blocks, the reverse process, *i.e.,* the

enzyme-catalytic transition from self-assemblies to their amorphous counterparts, can also be used to control the disassembly of Fmoc-modified self-assemblies.[95]

2.2.4.2. Kinetically driven self-assembly using biocatalysis

In addition to the thermodynamics-driven component selections in identification of stable self-assemblies, enzyme-triggered strategies can also be used to kinetically program ordered supermolecular Fmoc-modified self-associations.

When using subtilisin-catalytic hydrolysis of Fmoc-YL-OMe to prepare Fmoc-YL for hydrogelation, the supermolecular order expressed at molecular, nano- and micro-levels could be dramatically enhanced by simply increasing the enzyme concentrations, while maintaining a constant gelator concentration.[102] Studies have shown that the different concentration could alter the catalytic activity of subtilisin and the size of its clusters, which allowed the structurally diverse materials representing local free energy landscape minima to be dominantly accessed.[102] While when injecting the mixtures of urea and citric acid to Fmoc-LG solution containing urease, an autonomously self-regulating gel could be prepared.[103] Specifically, the citric acid acted as the activator, its ionization rapidly decreased the solution pH and formed a transient acidic pH state at which Fmoc-LG could self-assemble into rigid nanofibrillar hydrogels.[103] Following this, the slow enzyme-catalytic hydrolysis of urea to CO_2 and NH_3 (dormant deactivator) recovered the solution pH and induced the hydrogel feedback-driven self-melt. In specific, the biocatalysis rate was greatly dependent on the composition concentrations and the initial solution pH, resulting in a biocatalytic, programmable and switchable hydrogelation.[103]

The enzyme-catalytic thermodynamically and kinetically driven self-assembly strategies can offer opportunities to study the hierarchical process and relevant mechanisms underlying the self-assembly of Fmoc-modified biomolecules, along with diverse nanostructural morphologies and applications.

2.3. Fmoc-Modified tetra- and pentapeptides

Compared to individual amino acids or di- and tripeptides, less research has been focused on the self-assembly of Fmoc-modified longer oligopeptides, possibly because the influence of Fmoc on the self-assembly process will decrease as peptide sequences become longer. However, some tetra- and pentapeptides have certain specific functions, such as cell adhesion and specific binding. Fmoc modification of these kinds of sequences will likely endow versatile functionalities to the self-assemblies, as shown in Table 1.

Molecular simulations showed that Fmoc-RGDS and Fmoc-GRDS, two peptide sequences containing a fibronectin-derived cell adhesion sequence (RGD),[104] could both self-assemble to form parallel β-sheets at lower concentrations, driven by the interactions among Fmoc units.[105] However, at high concentrations, such as 1.0% (wt), Fmoc-RGDS formed antiparallel β-sheets since the parallel configuration was less stable as salt bridging played a significant role in self-assembly; while Fmoc-GRDS still retained parallel β-sheet arrangements.[106] Therefore, although both peptides self-assembled to form nanofibrillar hydrogels at higher concentrations, dynamic shear rheometry enabled the measurements of the moduli of the Fmoc-GRDS hydrogel, while synergism occurred for the Fmoc-RGDS hydrogel.[106] However, when replacing the S with F, Fmoc-RGDF and Fmoc-FRGD could both form rigid hydrogels, revealing the critical role of the side-chain aromatic moieties in the self-assembly process and subsequent physical properties of the hydrogels.[27,28]

Moreover, when modified by the Fmoc group, VTEEI (the repeat sequence in the *Plasmodium falciparum* blood stage antigen), GVGVP & VPGVG (peptide-based epitopes in elastin) and VYGGG (inhibitor in the binding monoclonal antibody 10D11) pentapeptide-based epitopes, could also self-assemble to form nanofibrillar hydrogels under the balance of intermolecular aromatic-aromatic interactions and hydrogen bonds.[107] The Fmoc-modified TIGYG, a potassium ion binding epitope derived from a natural ion-channel protein, could self-assemble to form nanofibers of varying widths and crosslinking patterns depending on the potassium concentrations used. In particular, hydrogelation could only happen at certain potassium *vs.* peptide ratios, confirming the conservation of the inherent ability of the epitopes to bind potassium ions.[22]

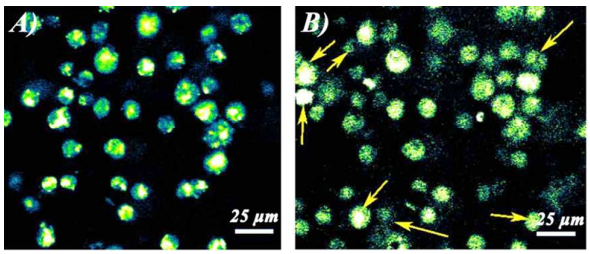

Figure 4. Laser confocal micrographs representing 3-D cultivating COS7 cells using *in situ* hydrogels self-assembled by Fmoc-FF as scaffolds: (A) 4 days and (B) 5 days of incubation. The arrows in (B) indicate the proliferated new cells. (Reproduced with permission from [108]. Copyright 2007 Springer)

3. Applications of the Fmoc-modified biomolecules

3.1. Cell culture scaffolds

Due to the excellent self-assembly and hydrogelation properties mentioned above, many studies have been devoted to the design and construction of cell culture systems using Fmoc-modified bio-assemblies,[9] which was recently specially reviewed by Xu and co-workers.[89] For example, during the cultivation of the mammalian cells including Astrocyte, MDCK and COS7 cells using Fmoc-FF hydrogels as 3-D scaffolds, low degree of growth was detected in the first 4 days while cell viability remained stable, as shown in Figure 4A.[108] Yet, after one more day of incubation, some cell migration and proliferation of new cells could be detected, as shown in

Figure 4B.[108] The biocompatible and degradable features of the hydrogel significantly reduced the cytotoxic effects present in traditional 3-D culture materials, and the ultrafast hydrogelation process simplified the microstructure-loading procedures.[108]

RGD-Based hydrogels can be used as an ideal cell culture support due to their intrinsic cell adhesion properties.[109] Through introduction of Fmoc-GRDS to a biomimetic collagen gel, the composite scaffold could enhance the adhesion and proliferation of viable human corneal stromal fibroblasts (hCSFs) by 300% compared to non-functionalized gels.[109] Furthermore, through incorporating Fmoc-RGDS self-assembling nanofibrils, the shrinkage of the collagen matrix gel was significantly suppressed due to the contractile action of encapsulated fibroblasts.[109] Moreover, the co-assembly of Fmoc-FF and Fmoc-RGD produced a bioactive hydrogel which could support 3-D cultures of human dermal fibroblasts. The encapsulated dermal fibroblasts could then deposit and organize the extracellular matrix (ECM) networks, including fibronectin and collagen I in a controlled manner.[111] The deposited ECM together with cell-assisted gel contraction endowed the cell-gel constructs with high rigidity. It should be noted that when removing Fmoc-RGD or replacing it with Fmoc-RGE, normal functions of fibroblasts including spreading, proliferation, ECM secretion and organization, were no longer detected, indicating that the RGD sequence is important for the *in vitro* dermal regeneration.[111]

3.2. Templates

Biomolecular self-assemblies have been widely studied as templates for low-dimensional assembly of functional composites due to their variable morphologies and tunable functionalities.[112-117] The ease of preparation in combination with the rigid stiffness of the Fmoc-modified self-assemblies, allow them to act as ideal bio-templates for the fabrication of nanomaterials. For example, Sn (IV) meso-tetra (4-pyridyl) porphine (SnTPyP) could be incorporated into the Fmoc-FF self-assembled nanofibers through electrostatic attraction interactions between the carboxyl and pyridyl groups, as shown in Figure 5A and 5B.[62] The efficiency and duration of visible light-driven oxygen evolution from photochemical oxidation of water molecules were dramatically increased via the excitation energy transfer (EET) of the assembled SnTPyP, which can be utilized to artificially mimic photosynthetic systems.[62] Furthermore, the acidic and polar moieties on the nanofibrillar surface could be utilized to mineralize $FePO_4$ by the sequential introduction of Fe^{3+} and PO_4^{3-}, as shown in Figure 5C. When heated to 350 °C, the $FePO_4$/nanofibril conjugates transformed to form $FePO_4$ nanotubes with inner walls coated with a thin layer of conductive carbon due to carbonization of the peptides, as shown in Figure 5D. These $FePO_4$ nanotubes were found to be promising cathode materials for rechargeable Li ion batteries, with a high reversible capacity and good stability during cycling.[118]

Another interesting work demonstrated that Fmoc-FFECG pentapeptide could self-assemble to form nanofibers possessing numerous carboxylic and thiol groups on their exterior, which could be used as templates for the mineralization of silver nanoparticles (Ag NPs). Moreover, it was found that the space- and size-constraint effects along with the physical isolation provided by the peptide nanofibers facilitated the monodispersity and stability of the Ag nanowires.[119] Interestingly, these Ag nanowires were shown to possess a highly effective and long-term antibacterial activity against both Gram-positive (*Bacillus subtilis*) and Gram-negative bacteria (*Escherichia coli DH5 α*), while being non-toxic to human cells.[119]

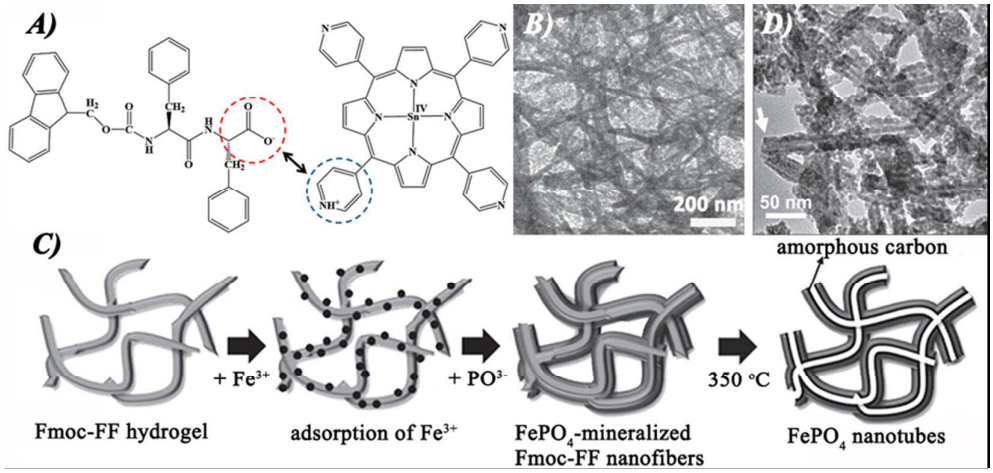

Figure 5. Fmoc-Modified self-assemblies as soft templates for nanocomposites organization. (A) Molecular structure and (B) TEM micrograph representing SnTPyP assembled along Fmoc-FF nanofibers with electrostatic attractive interactions. (Reproduced with permission from [62]. Copyright 2013 Wiley-VCH Verlag GmbH & Co. KGaA, Weinheim) (C) Schematic representation and (D) TEM micrograph showing the $FePO_4$ nanotubes produced using Fmoc-FF nanofibers as templates. The arrow in (D) denotes the terminus of a hollow $FePO_4$ nanotube. (Reproduced with permission from [118]. Copyright 2010 Wiley-VCH Verlag GmbH & Co. KGaA, Weinheim)

3.3. Optical properties

Considering the highly fluorescent and UV-active fluorenyl ring of the Fmoc group,[120,121] there is no doubt that the Fmoc-modified self-assemblies can exhibit distinct optical properties, which may be useful in various bionanotechnological fields.

3.3.1. Fluorescent properties and aggregation mechanisms. The remarkable fluorescence features of Fmoc, *i.e.,* the intense excitation at 270 nm and corresponding emission at 320 nm, can be used to characterize the synthesis and assembly process of Fmoc-modified biomolecules. For instance, when using the Fmoc solid phase peptide synthesis strategy to *in situ* synthesize peptides on a glass substrate and prepare a 2-D self-assembling bio-layer, the unique fluorescent properties of Fmoc could be used to monitor the amino acid coupling at individual stages. This methodology can supply a fast, inexpensive, and non-disruptive detection technique which is more accessible than conventional surface analytical characterizations.[122]

Furthermore, the fluorescent peak positions of the fluorenyl moiety can be utilized to probe the aggregation dynamics and associated nanostructural mechanism underlying the Fmoc-modified self-assemblies. Specifically, the wavelength bathochromic shift (red-shift) and hypsochromic shift (blue-shift) correspond to the formation of parallel-displaced J-aggregations[74] and face-to-face H-aggregations[78] of the aromatic moieties, respectively. For example, when dispersing Fmoc-modified 5-aminopentanoic acid (Fmoc-5), which has similar molecular dimensions to Fmoc-FF, in an acidic aqueous solution by a solvent-switching method, Fmoc-5 self-organized into plate-like crystals, in which the Fmoc groups exhibited a dominant emission peak at 324 nm red-shifting from its inherent fluorescence at 315 nm, corresponding to the formation of antiparallel arrangements. The spectral pattern did not change with time, indicating that the self-assemblies were considerably stable, as shown in Figure 6A.[123] While when adjusting the solution pH to basic, the Fmoc groups initially exhibited their inherent fluorescent emission as Fmoc-5 molecules were charged from deprotonation and remained at the monomeric state. Since Fmoc was gradually cleaved, a new emission peak at 467 nm emerged and dominated the fluorescence spectra, indicating that an extensive J-aggregation was formed, as shown in Figure 6B.[123] Furthermore, through the intensity ratio evolution at 467 nm and at 315 nm *vs.* time, the Fmoc groups aggregation dynamics at basic pH could be easily detected.[123]

3.3.2. Circular dichroism property and chiroptics. The ordered arrangements of the chiral amino acids and peptides can not only offer unique circular dichroism (CD) signals for investigating the molecular conformations of Fmoc-modified building blocks in the self-assemblies, but allow their molecular handedness to transit to the co-assembled optical moieties in the supermolecular structures, such as Fmoc, thus resulting in their inherent achiroptics to become chiral.

During Fmoc-GRDS self-assembly , the CD spectrum showed no signals in the Fmoc absorbance region (one centered at 265 nm and another one centered at 210 nm), suggesting that the Fmoc groups were not arranged in strongly ordered chiral structures.[124] In contrast, the linear dichroism spectrum was dominated by Fmoc units, showing a negative signal at 265 nm corresponding to the long axis of the Fmoc unit extending away from the fiber axis, while the 210 nm region was neither long-axis nor short-axis polarized. By symmetry, any one transition must be one of the two, indicating that this region of the spectrum is an overlay of different transitions.[124] The results suggest that the Fmoc units are approximately perpendicular to the fiber axis, with the long axis tilted somewhat more than the short axis.[124]

In fact, when using the biomolecular self-associations as soft templates to assemble optical components, their twisting handedness can induce the exciton coupling of the chiral array of chromophores, thus resulting in a bisignate band (Cotton effect) in the CD spectra.[125,126] Therefore, it is reasonable that the achiral Fmoc group could also show Cotton effect signals in the region of 270-310 nm corresponding to π-π* electron transitions, along with the CD signals of the peptides in the far-UV region (190-230 nm).[49,69,70,102] Furthermore, the polarity of the Cotton effect peaks, *i.e.,* the positive or negative signs of the ellipticity, can provide the information of the twisting orientations of the Fmoc and corresponding nanostructures, which is significantly useful for clarification of the self-assembly mechanims.[49,96] This strategy can be further utilized to assemble other achiroptical components, such as quantum dots,[127] surface plasmon resonant (SPR) metallic nanoparticles[128] and fluorescent dyes,[129] shedding light on future exploration of new nanomaterials with controllable chiroptics.

3.3.3. UV-vis absorption and semiconductivity. The self-assemblies of ultrashort peptides have been found to be able to show optical and electric properties comparable to conventional inorganic semiconductor materials.[4,130,131] For example, FF self-assembling nanotubes can exhibit remarkable luminescent,[132] piezoelectric[133] and mechanical properties,[134] due to the formation of quantum dots (QDs) within the nanostructures.[135] Undoubtedly, the introduction of the Fmoc moiety can further modulate the semiconductivity of the bio-assemblies and bring forth the next-generation semiconductor materials.[136,137]

UV-Vis spectroscopic analysis showed that the hydrogels formed by Fmoc-FF exhibited a pronounced step-like absorption pattern between 250 nm and 300 nm, accompanied by a peak at the long-wavelength edge (314 nm) derived from the strengthened Coulomb interaction of excitons, a characteristic of the formation of 2-D quantum well (QW) confinements.[138] The confined dimensions and reduced exciton mass were calculated to be 10 Å ≤ L_z ≤ 13.5 Å and $0.17m_0 \leq \mu \leq 0.2m_0$ (where L_z is the Z-dimension of the confined structure and μ is the reduced exciton mass), respectively, similar to those of traditional inorganic semiconductors.[138] Moreover, the hydrogel formed by Fmoc-2-Nal also showed a step-like absorption spectrum between 250 nm and 300 nm, with the estimated dimensions and reduced exciton mass of 9 Å ⩽ L_z ⩽ 12 Å and $0.3m_0 \leqslant \mu \leqslant 0.35m_0$,

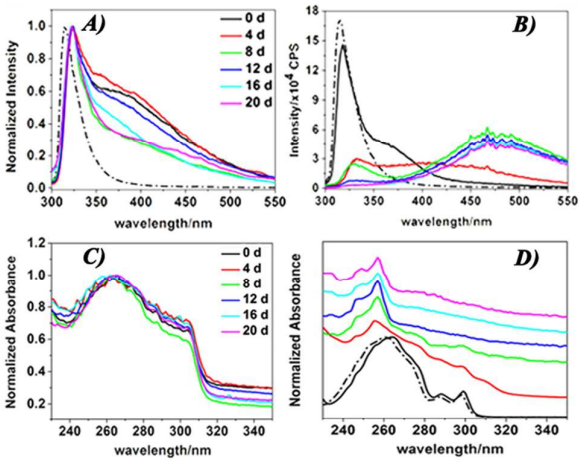

Figure 6. Fluorescence (A, B) and UV-vis absorbance (C, D) spectra of the Fmoc group modulated by pH-mediated self-assembly of Fmoc-5: (A, C) at pH 2.0, (B, D) at pH 10.0. Note that the spectrum of Fmoc-5 in HFIP was added and denoted as a dash-dot line as a control. (Reproduced with permission from [123]. Copyright 2015 Royal Society of Chemistry.)

respectively.[138] Therefore, it seems that the quantum confinement (QC) phenomenon is common to Fmoc-modified biomolecular self-assemblies; and the aromatic moieties, including the fluorenyl and side-chain phenyl groups, are probably the key parameters in determining the electronic QC properties.[53]

In addition to the influence of the Fmoc moiety on the self-assemblies, the organization of biomolecular backbones can also affect the optical properties of Fmoc. To investigate this influence while avoiding the potential effect of the intrinsic optical properties of the peptide backbones,[139] Fmoc-5 was chosen to serve as a simpler model without backbone contributions.[123] At pH 2.0, Fmoc-5 molecules formed plate-like crystals where Fmoc moieties were ordered in antiparallel arrangements and showed a step-like UV-vis absorbance from 260 nm to 300 nm, as shown in Figure 6C.[123] This implies that Fmoc groups form 2-D QW confined structures at this condition, probably with confined dimensions located along the Z-axis direction of the assemblies which is in the nanoscale range.[123] While at pH 10.0, as Fmoc was gradually cleaved and self-assembled to form 3-D bulky aggregates, a quasi-continuous absorbance emerged and dominated the UV-vis absorption spectra, as shown in Figure 6D.[123] Therefore, by simply modulating the solution pH, the QC type of Fmoc-modified self-assemblies can be controlled.

3.3.4. Infrared absorption and secondary structures. Due to the unique molecular geometries and hydrogen bonding patterns, each type of peptide secondary structures gives rise to a somewhat different vibration frequency in FTIR spectra. Therefore, along with CD, FTIR is another effective technique for characterization of biomolecular self-assembling secondary structures.[140] Among the IR peaks of interest, the amide I region (1700-1600 cm^{-1}, assigned to C=O bond stretching vibration) is substantially sensitive and can offer more information on the molecular conformations within the nanostructures.[141] It has been a common belief that the parallel and antiparallel β-sheet structures can be distinguished based on the analysis of the amide I region. In particular, in antiparallel β-sheet structures, the amide I region displays two typical components: the major component is located at ~1630 cm^{-1}, whereas the minor component is characterized at ~1695 cm^{-1}. For parallel β-sheet structures, the amide I region displays only the major component around 1630 cm^{-1}.[142] However, through comparison of the FTIR absorption of Fmoc-AA and its analogue, 9-fluorene-methylcarbonyl dialanine (Fmc-AA), with a combination of experimental and computational characterizations, it was found that the peak at ~1695 cm^{-1} is actually the adsorption of the stacked carbamate group, rather than the aforementioned characteristic of antiparallel β-sheet secondary structures.[25] This suggests that the previous conclusions of Fmoc-modified self-assemblies based on FTIR analysis needs to be re-analysed and updated.

3.4. Drug Delivery

Biomolecular self-assemblies have been widely studied as nanocarriers for encapsulation and delivery of drug molecules.[143-145] Nowadays, the development of advanced technologies, such as the precise medicine and nanobiotechnology, demands the nanocarriers to be easy for functionalization, such as integration with a specific target factor along with having the optimal encapsulation properties for hydrophobic drugs.[146,147] Due to the strong hydrophobicity of Fmoc and ease of modification of peptidic sequences, Fmoc-modified self-assemblies can serve the dual role of encapsulation and functionalization.

As a pioneering work of Fmoc-modified biomolecular hydrogelation, Fmoc-LD was designed to show the ability of forming a filamentous hydrogel with remarkable high elastic modulus and strain-weakening properties.[148] When entrapping low-molecular-weight drugs, *i.e.,* 3,5-dimethyl-ladamantmamine hydrochloride (AddMe) and 5-methyl-1-adamantanmine 3-carboxylic acid (Ada-MeC) which are inherently non-antigenic antiviral drugs, in the gel and injecting into rabbits, high titre specific antibodies were efficiently produced.[148] Compared with the traditional covalent conjugation of these drugs to biomacromolecular carriers such as bovine serum albumin (BSA), this entrapment approach permits simplicity in the preparation of antigenic aggregates, ease of standardization and excludes the need to chemically modify the hapten or use of an additional adjuvant, thus allowing the application of the Fmoc-modified hydrogels for antigen presentations.[148]

With the π-π interactions of the aromatic moieties (including Fmoc group and side-chain phenyl rings), Fmoc-FY dipeptide could wrap up the spherical nanoparticles self-assembled by Fmoc-tris(2-aminoethyl)amine (Fmoc-TAEA) and stabilize them at physiological pH in aqueous solution.[149] The two-component nanospheres were found to be stable upon heating, incubation

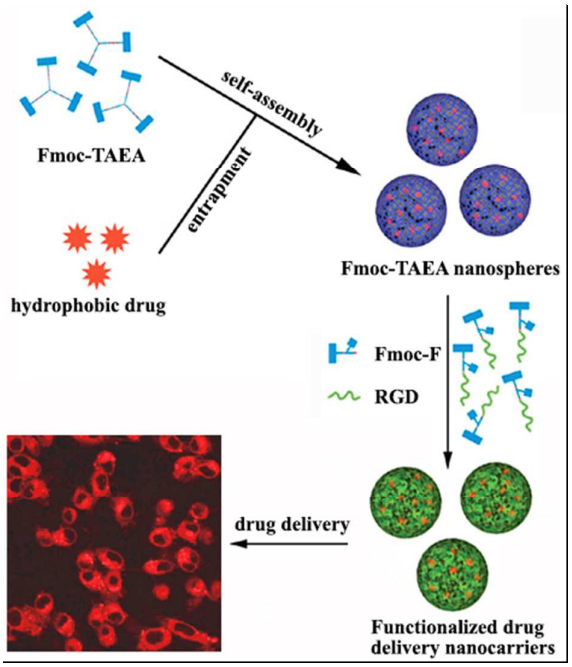

Figure 7. Schematic diagram of the construction of Fmoc-FRGD stabilized and functionalized Fmoc-TAEA self-assembling nanospheres, along with the entrapment of hydrophobic molecules for drug delivery. (Reproduced with permission from [150]. Copyright 2012 American Chemical Society.)

or dilution, and well-tolerated by cells (mouse embryonic fibroblast cells, NIH/3T3).[149,150] Moreover, through rational design based on three criteria (carrying Fmoc headgroup; the first amino acid with self-interacting side chain; net negative charge), another tetrapeptide, Fmoc-FRGD, was screened to show the same ability of stabilizing Fmoc-TAEA nanospheres.[150] Furthermore, the stabilized nanoparticles were capable of encapsulating hydrophobic dyes (Nile red) and targeting breast cancer cells (MDA-MB-435 cells), as shown in Figure 7.[150] This stepwise aromatic-driven self-assembly strategy can provide an elegant approach to construct functionalized and bioactive nanostructures with potential applications in diverse fields, such as active-targeting in drug delivery and directional bio-imaging in diagnostics.

3.5. Catalytic properties

Bio-inspired catalysts have become new hotspots in some cutting-edge research fields, such as the artificial-mimic enzymatic systems.[151-153] Due to the ease of morphological modulations and innate biocompatibility which endow the properties to be flexibly tuned and easily integrated into the biological world, biomolecular self-assemblies have been shown to present novel, next-generation enzymatic mimics. In this regard, the advantages of their fast association process, eminent stability and ease of modification, endow the Fmoc-modified self-assemblies efficient catalysis performance.

A previous study reported that Fmoc-FFH-NH_2 tripeptide could self-assemble to form nanotubes through a solvent-switching cycling from DMSO to water.[154] Taking advantage of the hydrophobic micro-environment provided by the Fmoc-FF segments and the catalytic center histidines (H) loaded on the periphery, the nanotubes exhibited a high catalytic activity for the hydrolysis of *p*-nitrophenyl acetate (PNPA).[154] Furthermore, through introducing Fmoc-FFR-NH_2, which contains a guanidyl group that can bind with the carbonyls, and then by optimizing the molar ratio of the catalytic centers and binding sites, the co-assembled nanotubes presented a much higher catalytic ability,[154] thus offering potential substitutes for natural hydrolases. In addition, through covalent conjugation of selenium (Se) with Fmoc-F, a hybridized Fmoc-F-Se selenide was synthesized to be able to self-assemble into nanospheres in an aqueous solution. The nanospheres showed a low catalytic activity for redox of glutathione (GSH) and hydroperoxides (ROOH), due to the fact that the catalytic Se sites were buried within the hydrophobic core of the nanostructures, as shown in Figure 8.[155] While following oxidation by hydroperoxides (ROOH), the selenide was quickly transformed into the selenoxide form, inducing the self-assembled morphologies to convert into nanotubes. This prompted the Se atoms to be exposed on the surface of the nanostructures, resulting in a much higher catalytic

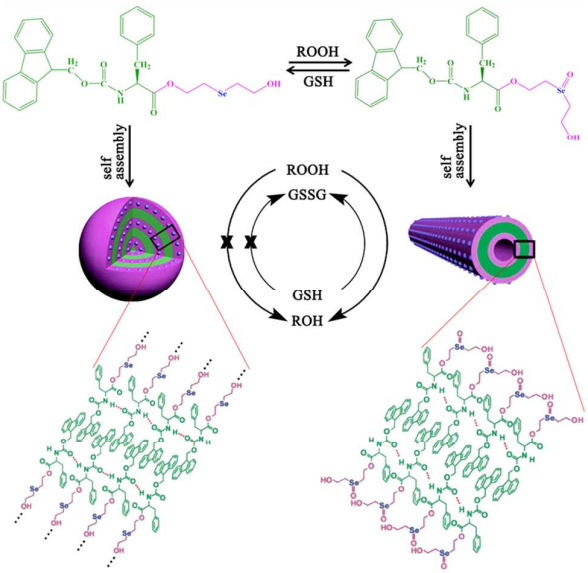

Figure 8. Redox-controlled Fmoc-F-Se molecular structures (upper panel); the reduced and oxidized conformation can self-assemble to nanospheres and nanotubes, respectively, inducing the catalytic Se buried within the hydrophobic core or exposed to the surface reversibly, resulting in switchable GPx catalytic activity (middle panel); the possible molecular arrangements of the nanostructures (lower panel). (Reproduced with permission from [155]. Copyright 2014 Royal Society of Chemistry.)

performance, as shown in Figure 8.[155] It should be noted that the phase transition and switchable catalytic activity are reversible, which make it possible to maintain the ROOH in an appropriate amount to allow the salutary function and avoid their harmful side effects.[155] The findings endow the Fmoc-F-Se self-assemblies with both an excellent sensor function to auto-detect the signal of ROOH and a smart enzymatic ability to controllably clear out superfluous ROOH through redox-induced morphological changes, which can be explored as artificial glutathione peroxidise (GPx) mimics in biosensor and biomedicine fields.

3.6. Therapeutic and antibiotic properties

Since their discovery over a decade ago, therapeutic and antibiotic peptides, such as antibacterial,[156,157] antifungal,[158] antiviral[159] and antitumoral[160] peptides, have attracted widespread interest.[89,161] However, the traditional bioactive peptides usually possess complicated molecular structures, which generally demand sophisticated extraction or synthesis procedures and are difficult to modulate. In comparison, Fmoc-modified biomolecules possess great advantages and can be considered as substitutes for their traditional counterparts.

In a pioneering study, several Fmoc-modified amino acids were found to possess a broad spectrum of antinflammatory activities, by blocking recruitment of neutrophils into inflammatory lesions and inhibiting T-cell activation when studied *in vitro*, rather than by traditionally inhibiting lipid metabolic enzymes or increasing the circulating levels of endogenous glucocorticoids.[162] Although the detailed action mechanism has yet remained unclarified, an important structural feature is that the more bulky the amino acid side chain, the greater their antinflammatory activity.[162] The results suggest that the Fmoc-modified single amino acids may be valuable therapeutic agents for inflammatory diseases.

With the help of the affinity chromatography method, the Fmoc-WFF tripeptide was screened to be an inhibitor to mouse ribonucleotide reductase (mRR), with a K_i similar to Ac-FTLDADF, a seven-amino acid oligopeptide inhibitor based on the C-terminal sequence of mRR.[163] The relatively smaller size and strong aromatic character make Fmoc-WFF a promising alternative for developing specific therapeutic inhibitors of mammalian RR.[163]

Fmoc-EXL-NH_2, where X represents phosphorylated Y mimetic, was found to exhibit high protein-tyrosine phosphatase (PTP) affinity properties. Specifically, when X was mono-anionic 4-(carboxydifluoromethyl)-F, Fmoc-EXL-NH_2 possessed an affinity equivalent to the di-anionic F2Pmp residue which have previously been among the most potent PTP-binding motifs.[164] However, when E was protected with an oxygen-butyl group (OBn) and X was 4-(carboxymethyloxy)-F, Fmoc-E(OBn)XL-NH_2 exhibited a high affinity to YopH (a virulence factor of *Yersinia pestis*), with a IC_{50} value as low as 2.8 μM.[164]

Fmoc-Modified Y-containing dipeptide, derived from inosine-catalytic dephosphorylation of the corresponding non-assembling phosphorylated esters, could self-assemble to form nanofibers *in vivo*, exhibiting potent antimicrobial potential.[165] Furthermore, when conjugating a pyridinium moiety to the C-terminal of Fmoc-FF, the cationic Fmoc-FF derivative exhibited efficient antibacterial activity against both Gram-positive (MIC of 25 μg mL^{-1} to *B. subtilis* and 10 μg mL^{-1} to *S. aureus*) and Gram-negative bacteria (MIC of 150 μg mL^{-1} to *E. coli* and 40 μg mL^{-1} to *P. aerugenosa*).[166] The antibacterial activity could be further modulated by changing the amino acid residues.[166]

4. Conclusions and Outlooks

In conclusion, Fmoc-modified amino acids and short peptides possess excellent self-assembly capabilities and exhibit eminent application potentials in a variety of fields. In this review, we summarized the recent advances regarding the self-assembly of these multifunctional bio-inspired molecules and described the relevant applications in cell cultivation, bio-templating, optics, drug delivery, biocatalysis, therapeutic and antibiotics in biomedical and bionanotechnological fields.

However, despite the extensive progress, there is yet much to be investigated. For instance, the Fmoc-modified self-assemblies are mainly 1-D nanofibers, leaving other morphologies far less studied. Moreover, to date their applications have been mostly focused on the hydrogelation and relevant mechanical properties, while other functions are still not well developed. Yet, it should be noted that these challenges also provide new opportunities. In the future, as novel modulation approaches are introduced, such as co-assembly, enzymatic triggering, modifications to the biomolecular structures, replacement of fluorenyl rings to heterocycles of the Fmoc group or addition of stimuli-responsive moieties, we believe that the challenges mentioned above will be solved, and the Fmoc-modified bio-assemblies will become pivotal contributors for human lives.

Acknowledgements

This work was supported in part by grants from the Israeli National Nanotechnology Initiative and the Helmsley Charitable Trust for a Focal Technology Area on Nanomedicine for Personalized Theranostics (E.G.). K.T. gratefully acknowledges the Center for Nanoscience and Nanotechnology of Tel Aviv University for financial support. The authors thank all the members of the Gazit laboratory for helpful discussions.

Notes and references

1 X. Gao and H. Matsui, *Adv. Mater.*, 2005, **17**, 2037.
2 S. G. Zhang, *Nat. Biotechnol.*, 2003, **21**, 1171.
3 X. B. Zhao, F. Pan, H. Xu, M. Yaseen, H. H. Shan, C. A. E. Hauser, S. G. Zhang and J. R. Lu, *Chem. Soc. Rev.*, 2010, **39**, 3480.
4 L. Adler-Abramovich and E. Gazit, *Chem. Soc. Rev.*, 2014, **43**, 6881.
5 F. Zhao, M. L. Ma and B. Xu, *Chem. Soc. Rev.*, 2009, **38**, 883.

6 R. V. Ulijn, and D. N. Woolfson, *Chem. Soc. Rev.,* 2010, **39**, 3349.
7 X. H. Yan, P. L. Zhu, and J. B. Li, *Chem. Soc. Rev.*, 2010, **39**, 1877.
8 D. J Adams, *Macromol. Biosci.*, 2011, **11**, 160.
9 D. M. Ryan, and B. L. Nilsson, *Polym. Chem.,* 2012, **3**, 18.
10 M. Zelzer, and Rein V. Ulijn, *Chem. Soc. Rev.,* 2010, **39**, 3351.
11 Z. Yang, G. L. Liang and B. Xu, *Acc. Chem. Res.*, 2008, **41**, 315.
12 R. V. Ulijn, *J. Mater. Chem.*, 2006, **16**, 2217.
13 L. Chen, S. Revel, K. Morris, L. C. Serpell and D. J. Adams, *Langmuir*, 2010, **26**, 13466.
14 Y. Zhang, Y. Kuang, Y. Gao and B. Xu, *Langmuir*, 2010, **27**, 529.
15 H. G. Cui, M. J. Webber and S. I. Stupp, *Biopolymers (Peptide Science)*, 2010, **94**, 1.
16 I. W. Hamley, *Chem. Commun.*, 2015, **51**, 8574.
17 L. A. Carpino and G. Y. Han, *J. Am. Chem. Soc.*, 1970, **92**, 2548.
18 L. A. Carpino and G. Y. Han, *J. Org. Chem.*, 1972, **37**, 3404.
19 L. A. Carpino, D. Sadat-Aalaee, H. G. Chao and R. H. DeSelms, *J. Am. Chem. Soc.*, 1990, **112**, 9651.
20 A. Mahler, M. Reches, M. Rechter, S. Cohen and E. Gazit, *Adv. Mater.*, 2006, **18**, 1365.
21 S. Fleming, S. Debnath, P. W. J. M. Frederix, T. Tuttle and R. V. Ulijn, *Chem. Commun.*, 2013, **49**, 10587.
22 Y. Kuang, Y. Gao, J. F. Shi, H. C. Lin and B. Xu, *Chem. Commun.*, 2011, **47**, 8772.
23 S. Fleming and R. V. Ulijn, *Chem. Soc. Rev.*, 2014, **43**, 8150.
24 R. J. Mart, R. D. Osborne, M. M. Stevens and R. V. Ulijn, *Soft Matter*, 2006, **2**, 822.
25 S. Fleming, P. W. J. M. Frederix, I. R. Sasselli, N. T. Hunt, R. V. Ulijn and T. Tuttle, *Langmuir*, 2013, **29**, 9510.
26 A. M. Smith, R. J. Williams, C. Tang, P. Coppo, R. F. Collins, M. L. Turner, A. Saiani and R. V. Ulijn, *Adv. Mater.*, 2008, **20**, 37.
27 R. Orbach, L. Adler-Abramovich, S. Zigerson, I. Mironi-Harpaz, D. Seliktar and E. Gazit, *Biomacromolecules*, 2009, **10**, 2646.
28 R. Orbach, I. Mironi-Harpaz, L. Adler-Abramovich, E. Mossou, E. P. Mitchell, V. T. Forsyth, E. Gazit and D. Seliktar, *Langmuir*, 2012, **28**, 2015.
29 S. Sutton, N. L. Campbell, A. I. Cooper, M. Kirkland, W. J. Frith and D. J. Adams, *Langmuir*, 2009, **25**, 10285.
30 D. M. Ryan, T. M. Doran, S. B. Anderson and B. L. Nilsson, *Langmuir*, 2011, **27**, 4029.
31 Z. M. Yang and B. Xu, *Chem. Commun.*, 2004, 2424.
32 A. Saha, S. Bolisetty, S. Handschin and R. Mezzenga, *Soft Matter*, 2013, **9**, 10239.
33 P. F. Caponi and R. V. Ulijn, *Polymers*, 2012, **4**, 1399.
34 G. Fichman, T. Guterman, J. Damron, L. Adler-Abramovich, J. Schmidt, E. Kesselman, L. J. W. Shimon, A. Ramamoorthy, Y. Talmon and E. Gazit, *Sci. Adv.*, 2016, 2, e1500827.
35 W. J. Frith, A. M. Donald, D. J. Adams and A. Aufderhorst-Roberts, *J. Non-Newton. Fluid*, 2015, **222**, 104.
36 D. M. Ryan, S. B. Anderson and B. L. Nilsson, *Soft Matter*, 2010, **6**, 3220.
37 Y. Q. Wang, Z. L. Zhang, L. Xu, X. Y. Li and H. Chen, *Colloid. Surface. B*, 2013, **104**, 163.
38 D. M. Ryan, S. B. Anderson, F. T. Senguen, R. E. Youngman and B. L. Nilsson, *Soft Matter*, 2010, **6**, 475.
39 Y. Liu, Y. Cheng, H. C. Wu, E. Kim, R. V. Ulijn, G. W. Rubloff, W. E. Bentley and G. F. Payne, *Langmuir*, 2011, **27**, 7380.
40 Y. Liu, E. Kim, R. V. Ulijn, W. E. Bentley and G. F. Payne, *Adv. Funct. Mater.*, 2011, **21**, 1575.
41 Y. Liu, J. L. Terrell, C. Y. Tsao, H. C. Wu, V. Javvaji, E. Kim, Y. Cheng, Y. F. Wang, R. V. Ulijn and S. R. Raghavan, *Adv. Funct. Mater.*, 2012, **22**, 3004.
42 K. Hanaoka, F. Qian, A. Boletta, A. K. Bhunia, K. Piontek, L. Tsiokas, V. P. Sukhatme, W. B. Guggino and G. G. Germino, *Nature*, 2000, **408**, 990.
43 A. H. Gröschel, A. Walther, T. I. Löbling, F. H. Schacher, H. Schmalz and A. H. E. Müller, *Nature*, 2013**, 503**, 247.
44 Z. M. Yang, H. W. Gu, Y. Zhang, L. Wang and B. Xu, *Chem. Commun.*, 2004, 208.
45 Z. M. Yang, K. M. Xu, L. Wang, H. W. Gu, H. Wei, M. J. Zhang and B. Xu, *Chem. Commun.*, 2005, 4414.
46 Z. M. Yang, L. Wang, J. Y. Wang, P. Gao and B. Xu, *J. Mater. Chem.*, 2010, **20**, 2128.
47 Q. G. Wang, Z. M. Yang, M. Ma, C. K. Chang and B. Xu, *Chem. -Eur. J.*, 2008, **14**, 5073.
48 D. M. Ryan, T. M. Doran and B. L. Nilsson, *Chem. Commun.*, 2011, **47**, 475.
49 D. M. Ryan, T. M. Doran and B. L. Nilsson, *Langmuir*, 2011, **27**, 11145.
50 B. Adhikari, J. Nanda and A. Banerjee, *Soft Matter*, 2011, **7**, 8913.
51 H. Cao, Q. Z. Yuan, X. F. Zhu, Y. P. Zhao and M. H. Liu, *Langmuir*, 2012, **28**, 15410.
52 X. M. Li, J. Y. Li, Y. Gao, Y. Kuang, J. F. Shi and B. Xu, *J. Am. Chem. Soc.*, 2010, **132**, 17707.
53 G. Rosenman, P. Beker, I. Koren, M. Yevnin, B. Bank-Srour, E. Mishina and S. Semin, *J. Pept. Sci.*, 2011, **17**, 75.
54 S. Kim, J. H. Kim, J. S. Lee and C. B. Park, *Small*, 2015, **11**, 3623.
55 P. W. J. M. Frederix, R. V. Ulijn, N. T. Hunt and T. Tuttle, *J. Phys. Chem. Lett.*, 2011, **2**, 2380.
56 P. W. J. M. Frederix, G. G. Scott, Y. M. Abul-Haija, D. Kalafatovic, C. G. Pappas, N. Javid, N. T. Hunt, R. V. Ulijn and T. Tuttle, *Nat. Chem.*, 2015, **7**, 30.
57 J. F. Shi, X. W. Du, Y. B. Huang, J. Zhou, D. Yuan, D. D. Wu, Y. Zhang, R. Haburcak, I. R. Epstein and B. Xu, *J. Am. Chem. Soc.*, 2015, **137**, 26.
58 E. K. Johnson, D. J. Adams and P. J. Cameron, *J. Am. Chem. Soc.*, 2010, **132**, 5130.
59 M. Reches and E. Gazit, *Science*, 2003, **300**, 625.
60 J. Raeburn, G. Pont, L. Chen, Y. Cesbron, R. Lévy and D. J. Adams, *Soft Matter*, 2012, **8**, 1168.
61 C. Tang, A. M. Smith, R. F. Collins, R. V. Ulijn and A. Saiani, *Langmuir*, 2009, **25**, 9447.
62 J. H. Kim, D. H. Nam, Y. W. Lee, Y. S. Nam and C. B. Park, *Small*, 2014, **10**, 1272.
63 H. -G. Braun and A. Z. Cardoso, *Colloids Surf. B*, 2012, **97**, 43.
64 J. Raeburn, C. Mendoza-Cuenca, B. N. Cattoz, M. A. Little, A. E. Terry, A. Z. Cardoso, P. C. Griffiths and D. J. Adams, *Soft Matter*, 2015, **11**, 927.
65 W. Helen, P. d. Leonardis, R. V. Ulijn, J. Gough and N. Tirelli, *Soft Matter*, 2011, **7**, 1732.
66 V. Jayawarna, S. M. Richardson, A. R. Hirst, N. W. Hodson, A. Saiani, J. E. Gough and R. V. Ulijn, *Acta Biomater.*, 2009, **5**, 934.
67 M. Zhou, A. M. Smith, A. K. Das, N. W. Hodson, R. F. Collins, R. V. Ulijn and J. E. Gough, *Biomaterials*, 2009, **30**, 2523.
68 G. Pont, L. Chen, D. G. Spiller and D. J. Adams, *Soft Matter*, 2012, **8**, 7797.
69 S. Roy, N. Javid, P. W. J. M. Frederix, D. A. Lamprou, A. J. Urquhart, N. T. Hunt, P. J. Halling and R. V. Ulijn, *Chem. – Eur. J.*, 2012, **18**, 11723.
70 S. Roy, N. Javid, J. Sefcik, P. J. Halling and R. V. Ulijn, *Langmuir*, 2012, **28**, 16664.
71 C. G. Pappas, T. Mutas, P. W. J. M. Frederix, S. Fleming, S. Bai, S. Debnath, S. M. Kelly, A. Gachagan and R. V. Ulijn, *Mater. Horiz.*, 2015, **2**, 198.
72 S. Bai, C. Pappas, S. Debnath, P. W. J. M. Frederix, J. Leckie, S. Fleming and R. V. Ulijn, *ACS Nano*, 2014, **8**, 7005.

73 S. Fleming, S. Debnath, P. W. J. M. Frederix, N. T. Hunt and R. V. Ulijn, *Biomacromolecules*, 2014, **15**, 1171.
74 C. Tang, R. V. Ulijn and A. Saiani, *Langmuir*, 2011, **27**, 14438.
75 C. Tang, R. V. Ulijn and A. Saiani, *Eur. Phys. J. E*, 2013, **36**, 1.
76 G. Fichman, L. Adler-Abramovich, S. Manohar, I. Mironi-Harpaz, T. Guterman, D. Seliktar, P. B. Messersmith and E. Gazit, *ACS Nano*, 2014, **8**, 7220.
77 H. Shao, T. Nguyen, N. C. Romano, D. A. Modarelli and J. R. Parquette, *J. Am. Chem. Soc.*, 2009, **131**, 16374.
78 H. Sha and J. R. Parquette, *Chem. Commun.*, 2010, **46**, 4285.
79 G. Cheng, V. Castelletto, C. M. Moulton, G. E. Newby and I. W. Hamley, *Langmuir*, 2010, **26**, 4990.
80 Y. Y. Xie, X. C. Wang, R. L. Huang, W. Qi, Y. F. Wang, R. X. Su and Z. M. He, *Langmuir*, 2015, **31**, 2885.
81 Y. Zhang, H. W. Gu, Z. M. Yang and B. Xu, *J. Am. Chem. Soc.*, 2003, **125**, 13680.
82 D. Bardelang, F. Camerel, J. C. Margeson, D. M. Leek, M. Schmutz, M. B. Zaman, K. Yu, D. V. Soldatov, R. Ziessel, C. I. Ratcliffe, and J. A. Ripmeester, *J. Am. Chem. Soc.*, 2008, **130**, 3313.
83 Y. Wang, C. Zhan, H. Fu, X. Li, X. Sheng, Y. Zhao, D. Xiao, Y. Ma, J. S. Ma and J. Yao, *Langmuir*, 2008, **24**, 7635.
84 X. J. Mu, K. M. Eckes, M. M. Nguyen, L. J. Suggs and P. Y. Ren, *Biomacromolecules*, 2012, **13**, 3562.
85 I. R. Sasselli, R. V. Ulijn and T. Tuttle, *Phys. Chem. Chem. Phys.*, 2016, **18**, 4659.
86 D. J Adams, L. M. Mullen, M. Berta, L. Chen, W. J. Frith, *Soft Matter*, 2010, **6**, 1971.
87 Z. M. Yang and B. Xu, *J. Mater. Chem.*, 2007, **17**, 2385.
88 R. V Ulijn and A. M. Smith, *Chem. Soc. Rev.*, 2008, **37**, 664.
89 X. Du, J. Zhou, J. Shi, and B. Xu, *Chem. Rev.* 2015, **115**, 13165.
90 M. Hughes, P. W. J. M. Frederix, J. Raeburn, L. S. Birchall, J. Sadownik, F. C. Coomer, I. H. Lin, E. J. Cussen, N. T. Hunt, T. Tuttle, S. J. Webb, D. J. Adams and R. V. Ulijn, *Soft Matter*, 2012, **8**, 5595.
91 M. Hughes, L. S. Birchall, K. Zuberi, L. A. Aitken, S. Debnath, N. Javid and R. V. Ulijn, *Soft Matter*, 2012, **8**, 11565.
92 S. Toledano, R. J. Williams, V. Jayawarna and R. V. Ulijn, *J. Am. Chem. Soc.*, 2006, **128**, 1070.
93 H. X. Xu, A. K. Das, M. Horie, M. S. Shaik, A. M. Smith, Y. Luo, X. F. Lu, R. Collins, S. Y. Liem and A. Song, *Nanoscale*, 2010, **2**, 960.
94 R. J. Williams, A. M. Smith, R. Collins, N. Hodson, A. K. Das and R. V. Ulijn, *Nat. Nanotechnol.*, 2009, **4**, 19.
95 A. K. Das. R. Collins and R. V. Ulijn, *Small*, 2008, **4**, 279.
96 C. G. Pappas, Y. M. Abul-Haija, A. Flack, P. W. J. M. Frederix and R. V. Ulijn, *Chem. Commun.*, 2014, **50**, 10630.
97 M. Hughes, H. X. Xu, P. W. J. M. Frederix, A. M. Smith, N. T. Hunt, T. Tuttle, I. A. Kinloch and R. V. Ulijn, *Soft Matter*, 2011, **7**, 10032.
98 J. W. Sadownik and R. V. Ulijn, *Chem. Commun.*, 2010, **46**, 3481.
99 L. Chronopoulou, S. Lorenzoni, G. Masci, M. Dentini, A. R. Togna, G. Togna, F. Bordi and C. Palocci, *Soft Matter*, 2010, **6**, 2525.
100 J. W. Sadownik, J. Leckie and R. V. Ulijn, *Chem. Commun.*, 2011**, 47**, 728.
101 W. P. Wang, Z. M. Yang, S. Patanavanich, B. Xu and Y. Chau, *Soft Matter*, 2008, **4**, 1617.
102 A. R. Hirst, S. Roy, M. Arora, A. K. Das, N. Hodson, P. Murray, S. Marshall, N. Javid, J. Sefcik, J. Boekhoven, J. H. v. Esch, S. Santabarbara, N. T. Hunt and R. V. Ulijn, *Nature Chem.*, 2010, **2**, 1089.
103 T. Heuser, E. Weyandt and A. Walther, *Angew. Chem. Int. Ed.,* 2015, **54**, 13258.
104 A. C. Mendes, E. T. Baran, R. L. Reis and H. S. Azevedo, *Wiley Interdiscipl. Rev. Nanomed. Nanobiotechnol.*, 2013, **5**, 582.
105 D. E. López-Pérez, G. Revilla-López, I. W. Hamley and C. Alemán, *Soft Matter*, 2013, **9**, 11021.
106 V. Castelletto, C. M. Moulton, G. Cheng, I. W. Hamley, M. R. Hicks, A. Rodger, D. E. López-Pérez, G. Revilla-López and C. Alemán, *Soft Matter*, 2011, **7**, 11405.
107 M. L. Ma, Y. Kuang, Y. Gao, Y. Zhang, P. Gao and B. Xu, *J. of Am. Chem. Soc.*, 2010, **132**, 2719.
108 T. Liebmann, S. Rydholm, V. Akpe and H. Brismar, *BMC Biotechnol.*, 2007, **7**, 88.
109 G. Cheng, V. Castelletto, R. R. Jones, C. J. Connon and I. W. Hamley, *Soft Matter*, 2011, **7**, 1326.
110 R. M. Gouveia, R. R. Jones, I. W. Hamley and C. J. Connon, *Biomater. Sci.*, 2014, **2**, 1222.
111 M. Zhou, R. V. Ulijn and J. E. Gough, *J. Tissue Eng.*, 2014, **5**, 2041731414531593.
112 M. S. Lamm, N. Sharma, K. Rajagopal, F. L. Beyer, J. P. Schneider and D. J. Pochan, *Adv. Mater.*, 2008, **20**, 447.
113 E. Kasotakis, E. Mossou, L. Adler-Abramovich, E. P. Mitchell, V. T. Forsyth, E. Gazit and A. Mitraki, *Biopolymers (Peptide Science)*, 2009, **92**, 164
114 K. Tao, J. Q. Wang, Y. P. Li, D. H. Xia, H. H. Shan, H. Xu and J. R. Lu, *Sci. Rep.*, 2013, **3**, 2565.
115 C. L. Chen, P. J. Zhang and N. L. Rosi, *J. Am. Chem. Soc.*, 2008, **130**, 13555.
116 J. D. Hartgerink, E. Beniash and S. I. Stupp, *Science*, 2001, **294**, 1684.
117 R. D. L. Rica, E. Mendoza and H. Matsui, *Small*, 2010, **6**, 1753.
118 J. Ryu, S. W. Kim, K. Kang and C. B. Park, *Adv. Mater.*, 2010, **22**, 5537.
119 Y. G. Wang, L. Cao, S. W. Guan, G. N. Shi, Q. Luo, L. Miao, I. Thistlethwaite, Z. P. Huang, J. Y. Xu and J. Q. Liu, *J. Mater. Chem.*, 2012, **22**, 2575.
120 A. R. Morales, C. O. Yanez, K. J. Schafer-Hales, A. I. Marcus and K. D. Belfield, *Bioconjugate Chem.*, 2009, **20** , 1992.
121 K. J. Schafer-Hales, K. D. Belfield, Y. Sheng, P. K. Frederiksen, J. M. Hales and P. E. Kolattukudy, *J. Biomed. Opt.*, 2005, **10** , 051402.
122 M. Zelzer, D. J. Scurr, M. R. Alexander and R. V. Ulijn, *ACS Appl. Mater. Interfaces*, 2012, **4**, 53.
123 K. Tao, E. Yoskovitz, L. Adler-Abramovich and E. Gazit, *RSC Adv.*, 2015, **5**, 73914.
124 Y. Zou, K. Razmkhah, N. P. Chmel, I. W. Hamley and A. Rodger, *RSC Adv.*, 2013, **3**, 10854.
125 F. D. Lewis, L. Zhang, X. Liu, X. Zuo, D. M. Tiede, H. Long and G. C. Schatz, *J. Am. Chem. Soc.*, 2005, **127**, 14445.
126 S. G. Telfer, T. M. McLean and M. R. Waterland, *Dalton Trans.*, 2011, **40**, 3097.
127 J. Yeom, B. Yeom, H. Chan, K. W. Smith, S. Dominguez-Medina, J. H. Bahng, G. Zhao, W. -S. Chang, S. -J. Chang, A. Chuvilin, D. Melnikau, A. L. Rogach, P. Zhang, S. Link, P. Král and N. A. Kotov, *Nature Mater.*, 2015, **14**, 66.
128 C. Song, M. G. Blaber, G. Zhao, P.n Zhang, H. C. Fry, G. C. Schatz and N. L. Rosi, *Nano Lett.*, 2013, **13**, 3256.
129 H. C. Fry, J. M. Garcia, M. J. Medina, U. M. Ricoy, D. J. Gosztola, M. P. Nikiforov, L. C. Palmer and S. I. Stupp, *J. Am. Chem. Soc.*, 2012, **134**, 14646.
130 B. Akdim, R. Pachter and R. R. Naik, *Appl. Phys. Lett.*, 2015, **106**, 183707.
131 Z. Fan, L. Sun,Y. Huang, Y. Wang and M. Zhang, *Nature Nanotechno.*, 2016, doi:10.1038/nnano.2015.312.
132 N. Amdursky, M. Molotskii, D. Aronov, L. Adler-Abramovich, E. Gazit and G. Rosenman, *Nano Lett.*, 2009, **9**, 3111.
133 A. Kholkin, N. Amdursky, I. Bdikin, E. Gazit and G. Rosenman, *ACS Nano*, 2010, **4**, 610.

134 L.Adler-Abramovich, N. Kol, I. Yanai, D. Barlam, R. Z. Shneck, E. Gazit and I. Rousso, *Angew. Chem., Int. Ed.*, 2010, **49**, 9939.
135 N. Amdursky, M. Molotskii, E. Gazit and G. Rosenman, *J. Am. Chem. Soc.*, 2010, **132**, 15632.
136 E. Gazit, *Nature Nanotechno.*, 2016, doi:10.1038/nnano.2015.321.
137 C. A. E. Hauser and S. Zhang, *Nature*, 2010, **468**, 516.
138 N. Amdursky, E. Gazit and G. Rosenman, *Adv. Mater.*, 2010, **22**, 2311.
139 D. Pinotsi, A. K. Buell, C. M. Dobson, G. S. K. Schierle and C. F. Kaminski, *ChemBioChem*, 2013, **14**, 846.
140 D. M. Byler and H. Susi, *Biopolymers*, 1986, **25**, 469.
141 J. Kong and S. N. Yu, *Acta Biochim. Biophys. Sinica*, 2007, **39**, 549.
142 E. Cerf, R. Sarroukh, S. Tamamizu-Kato, L. Breydo, S. Derclaye, Y. F. Dufrêne, V. Narayanaswami, E. Goormaghtigh, J. -M. Ruysschaert and V. Raussens, *Biochem. J.*, 2009, **421**, 415.
143 T. M. Allen and P. R. Cullis, *Science*, 2004, **303**, 1818.
144 K. Kataoka, A. Harada and Y. Nagasaki, *Adv. Drug Deliv. Rev.*, 2001, **47**, 113.
145 A. Rösler, G. W. M. Vandermeulen and H. -A. Klok, *Adv. Drug Deliv. Rev.*, 2012, **64**, 270.
146 S. S. Dharap, Y. Wang, P. Chandna, J. J. Khandare , B. Qiu, S. Gunaseelan, P. J. Sinko, S. Stein, A. Farmanfarmaian and T. Minko, *Proc. Natl. Acad. Sci. USA*, 2005, **102**, 12962.
147 K. Cho, X. Wang, S. Nie, Z. Chen and D. M. Shin, *Clin. Cancer Res.*, 2008, **14**, 1310.
148 R. Vegners, I. Shestakova, I. Kalvinsh, R. M. Ezzell and P. A. Janmey, *J. Pept. Sci.*, 1995, **1**, 371.
149 W. Wang and Y. Chau, *Chem. Commun.*, 2011, **47**, 10224.
150 W. Wang and Y. Chau, *Chem. Mater.*, 2012, **24**, 946.
151 R. Breslo, *Acc. Chem. Res.*, 1995, **28**, 146.
152 M. Raynal, P. Ballester, A. Vidal-Ferran and P. W. N. M. v. Leeuwen, *Chem. Soc. Rev.*, 2014, **43**, 1734.
153 W. B. Motherwell, M. J. Bingham and Y. Six, *Tetrahedron*, 2001, **57**, 4663.
154 Z. Huang, S. Guan, Y. Wang, G. Shi, L. Cao, Y. Gao, Z. Dong, J. Xu, Q. Luo and J. Liu, *J. Mater. Chem. B*, 2013, **1**, 2297.
155 Z. Huang, Q. Luo, S. Guan, J. Gao, Y. Wang, B. Zhang, L. Wang, J. Xu, Z. Dong and J. Liu, *Soft Matter*, 2014, **10**, 9695.
156 V. Nizet, T. Ohtake, X. Lauth, J. Trowbridge, J. Rudisill, R. A. Dorschner, V. Pestonjamasp, J. Piraino, K. Huttner and R. L. Gallo, *Nature*, 2001, **414** , 454.
157 S. Fernandez-Lopez, H. -S. Kim, E. C. Choi, M. Delgado, J. R. Granja, A. Khasanov, K. Kraehenbuehl, G. Long, D. A. Weinberger, K. M. Wilcoxen and M. R. Ghadiri, *Nature*, 2001, **412**, 452.
158 C. H. Park, E. V. Valore, A. J. Waring and T. Ganz, *J. Biol. Chem.*, 2001, **276**, 7806.
159 M. Y. Zeng, W. X. Cui, Y. H. Zhao, Z. Y. Liu, S. Y. Dong and Y. Guo, *Chin. J. Oceanol. Limn.*, 2008, **26**, 307.
160 Y. F. Liu, J. Hu, J. H. Zhang, S. L. Wang and C. F. Wu, *Prep. Biochem. Biotech.*, 2002, **32**, 317.
161 M. Zasloff, *Nature*, 2002, **415**, 389.
162 R. M. Burch, M. Weitzberg, N. Blok, R. Muhlhauser, D. Martin, S. G. Farmer, J. M. Bator, J. R. Connor, M. Green and C. Ko, *Proc. Natl. Acad. Sci. USA*, 1991, **88**, 355.
163 Y. Gao, S. Liehr and B. S. Cooperman, *Bioorg. Med. Chem. Lett.*, 2002, **12**, 513.
164 K. Lee, Y. Gao, Z. J. Yao, J. Phan, L. Wu, J. Liang, D. S. Waugh, Z. Y. Zhang and T. R. Burke, *Bioorg. Med. Chem. Lett.*, 2003, **13**, 2577.
165 M. Hughes, S. Debnath, C. W. Knapp and R. V. Ulijn, *Biomater. Sci.*, 2013, **1**, 1138.
166 S. Debnath, A. Shome, D. Das and P. K. Das, *J. Phys. Chem. B*, 2010, **114**, 4407.
167 Z. M. Yang, H. W. Gu, D. G. Fu, P. Gao, J. K. Lam and B. Xu, *Adv. Mater.*, 2004, **16**, 1440.